Atmos. Meas. Tech. Discuss., doi:10.5194/amt-2016-78, 2016
Manuscript under review for journal Atmos. Meas. Tech.
Published: 7 April 2016

Atmospheric Measurement Techniques Discussions

Evaluation of NO^+ reagent ion chemistry for on-line measurements of atmospheric volatile organic compounds

Abigail R. Koss[1,2,3], Carsten Warneke[1,2], Bin Yuan[1,2], Matthew M. Coggon[1,2], Patrick R. Veres[1,2], Joost A. de Gouw[1,2,3]

1. NOAA Earth System Research Laboratory (ESRL), Chemical Sciences Division, Boulder, CO, USA

2. Cooperative Institute for Research in Environmental Sciences, University of Colorado at Boulder, Boulder, CO, USA

3. Department of Chemistry and Biochemistry, University of Colorado at Boulder, CO, USA

Atmos. Meas. Tech. Discuss., doi:10.5194/amt-2016-78, 2016
Manuscript under review for journal Atmos. Meas. Tech.
Published: 7 April 2016

Atmospheric Measurement Techniques Discussions

10 **Abstract**

11 NO^+ chemical ionization mass spectrometry (NO^+ CIMS) can achieve fast (sub 1-Hz) on-
12 line measurement of trace atmospheric volatile organic compounds (VOCs) that cannot be ionized
13 with H_3O^+ ions (e.g. in a PTR-MS or H_3O^+ CIMS instrument). Here we describe the adaptation of
14 a high-resolution time-of-flight H_3O^+ CIMS instrument to use NO^+ primary ion chemistry. We
15 evaluate the NO^+ technique with respect to compound specificity, sensitivity, and VOC species
16 measured compared to H_3O^+. The evaluation is established by a series of experiments including
17 laboratory investigation using a gas-chromatography (GC) interface, in-situ measurement of urban
18 air using a GC interface, and direct in-situ measurement of urban air. The main findings are that
19 (1) NO^+ is useful for isomerically resolved measurements of carbonyl species; (2) NO^+ can achieve
20 sensitive detection of small (C4-C8) branched alkanes, but is not unambiguous for most; and (3)
21 compound-specific measurement of some alkanes, especially iso-pentane, methylpentanes, and
22 high mass (C12-C15) n-alkanes, is possible with NO^+. We also demonstrate fast in-situ chemically
23 specific measurements of C12 to C15 alkanes in ambient air.

24

25 Keywords: NO^+, chemical ionization mass spectrometry, VOCs, atmosphere, PTRMS

Atmos. Meas. Tech. Discuss., doi:10.5194/amt-2016-78, 2016
Manuscript under review for journal Atmos. Meas. Tech.
Published: 7 April 2016

Atmospheric Measurement Techniques Discussions

1. Introduction

Volatile organic compounds (VOCs) are central to the formation of ozone and secondary organic aerosol (SOA), and can have direct human health effects. Understanding the behavior of these species in the troposphere presents several measurement challenges (Glasius and Goldstein, 2016). First, VOCs are highly chemically diverse. Second, many environmentally important species require measurement precision of better than 100 parts-per-trillion (ppt). Finally, numerous applications, such as eddy flux analyses or sampling from a mobile platform, require fast in-situ measurements, with sub-1 minute time resolution.

H_3O^+ chemical ionization mass spectrometry (H_3O^+ CIMS) , more commonly known as proton-transfer-reaction mass spectrometry (PTR-MS), is a well-established approach to measuring VOCs (de Gouw and Warneke, 2007;Jordan et al., 2009b). In H_3O^+ CIMS, air is mixed with hydronium (H_3O^+) ions in a drift tube region. VOCs are ionized by transfer of the proton from H_3O^+ to the VOC. These instruments are capable of VOC measurements that are fast, sensitive, and chemically detailed (Jordan et al., 2009b;Graus et al., 2010;Sulzer et al., 2014;Yuan et al., 2016).

Despite these advantages, H_3O^+ CIMS has several limitations related to the reagent ion chemistry. For one, this technique generally cannot distinguish between isomers. For instance, this is a significant limitation when measuring aldehyde and ketone carbonyl isomers, which have very different behavior in the atmosphere. Separation of propanal and acetone with PTRMS has been explored using collision-induced dissociation with an ion-trap mass analyzer, but this technique negatively affects the instrument time resolution and sensitivity (Warneke et al., 2005). Additionally, some proton transfer reactions are dissociative. Large hydrocarbons (C8 and larger) fragment into common small masses, making spectra difficult to interpret (Jobson et al., 2005;Erickson et al., 2014;Gueneron et al., 2015). Alcohols and aldehydes can lose H_2O, lowering the sensitivity to the protonated parent mass; their product ion masses then coincide with those of hydrocarbons, making independent measurement difficult (Španěl et al., 1997;Buhr et al., 2002). Furthermore, H_3O^+ CIMS is not sensitive to small (~C8 and smaller) saturated alkanes, as their proton affinities are lower than or very close to that of water (Arnold et al., 1998;Gueneron et al., 2015). This is a serious limitation in studies of urban air or emissions from oil and natural gas extractions, where small alkanes can contribute a large fraction to the total gas phase carbon and

Atmos. Meas. Tech. Discuss., doi:10.5194/amt-2016-78, 2016
Manuscript under review for journal Atmos. Meas. Tech.
Published: 7 April 2016

Atmospheric Measurement Techniques Discussions

chemical reactivity (Katzenstein et al., 2003;Gilman et al., 2013). Gas chromatography techniques avoid many of these limitations, but have much slower time resolution.

Use of NO^+ reagent ion chemistry may address some of the limitations of H_3O^+. Reaction of NO^+ with various VOCs has been extensively studied using selected-ion flow tube methods (SIFT-MS). SIFT methods use a quadrupole mass filter in between the ion source and ion-molecule reactor, which provides a very pure reagent ion source but limits the primary ion signal. SIFT studies have identified the major products of the reaction of NO^+ with VOCs representative of many different functional groups (Španěl and Smith, 1996, 1998a, b, 1999;Španěl et al., 1997;Arnold et al., 1998;Francis et al., 2007a;Francis et al., 2007b). Aldehydes and ketones are easily separable: ketones cluster with NO^+, forming mass (m+30) ions, whereas aldehydes react by hydride abstraction, forming mass (m-1) ions (where m is the molecular mass of the species). Rather than losing H_2O, as in H_3O^+ CIMS, alcohols react by NO^+ adduct formation or hydride abstraction. And finally, NO^+ can be used to detect alkanes: small (>C4) branched alkanes and large (>C8) n-alkanes react by hydride abstraction, forming mass (m-1).

The application of SIFT methods to atmospheric analysis has been limited by relatively poor sensitivity (Smith and Španěl, 2005;Francis et al., 2007b;de Gouw and Warneke, 2007); although better sensitivities have been reported in recent years (Prince et al., 2010). The adaptation of an existing CIMS instrument to use the SIFT technique requires extensive instrument modification or the purchase of an external SIFT unit (Karl et al., 2012). Several groups have experimented with low-cost adaptation of H_3O^+ CIMS instruments to use NO^+ chemistry. Knighton et al. (2009) adapted an H_3O^+ CIMS instrument to measure 1,3-butadiene and demonstrated in-situ detection of this species in the atmosphere. Jordan et al. (2009a) have developed a hollow-cathode ion source capable of switchable reagent ion chemistry, and demonstrated laboratory measurement with NO^+ of several aromatics, chlorinated aromatics, and carbonyls, with sensitivities comparable to H_3O^+ CIMS. The NO^+ capability of the Jordan et al. instrument has been used in the laboratory by Inomata et al. (2013) to investigate detection of n-tridecane and by Agarwal et al. (2014) to measure picric acid, and by Liu et al. (2013) to investigate the behavior of MVK and methacrolein in a reaction chamber.

These studies suggest that an easy, low-cost adaptation of H_3O^+ CIMS instruments to NO^+ chemistry could greatly enhance our capability to measure VOCs in the atmosphere. However, the number of VOC species investigated to-date is small and few field measurements have been

Atmos. Meas. Tech. Discuss., doi:10.5194/amt-2016-78, 2016
Manuscript under review for journal Atmos. Meas. Tech.
Published: 7 April 2016

reported. The ability of a modified H_3O^+ CIMS instrument to separate carbonyl isomers in ambient air, and to measure small alkanes both in the laboratory and in ambient air, has not been evaluated. Finally, the lack of fragmentation of n-tridecane reported in Inomata et al. (2013) is intriguing, but the use of an NO^+ CIMS instrument to measure similar high-mass alkanes in ambient air has not been demonstrated.

Here we evaluate the adaptation of an H_3O^+ CIMS instrument to use NO^+ reagent ion chemistry. We provide specifics on instrument set-up and operating parameters. We report the sensitivity and spectral simplicity of NO^+ CIMS, relative to H_3O^+ CIMS, for nearly 100 atmospherically relevant VOCs, including a wide range of functional groups, and provide product ion distributions for several representative compounds. We demonstrate, interpret, and evaluate measurements of separate aldehyde and ketone isomers, light alkanes, and several other species in ambient air. Finally, we investigate measurement of high-molecular-mass alkanes using NO^+. We extend the laboratory analysis of high-mass alkanes to C12-C15 n-alkanes and demonstrate fast, in-situ measurement of these species in ambient air.

2. Methods

2.1 Instrumentation

Two separate H_3O^+ CIMS instruments (referred to hereafter as PTR-QMS and H_3O^+ ToF-CIMS) were adapted to NO+ chemistry in this work. Both instruments consist of (1) a hollow cathode reagent ion source, (2) a drift tube reaction region, (3) an ion transfer stage that transports from the drift tube to the mass analyzer and allows differential pumping, and (4) a mass analyzer. Both instruments have nearly identical hollow cathode ion sources and drift tube reaction regions, described in detail in de Gouw and Warneke (2007). The PTR-QMS (Ionicon Analytik) uses ion lenses to transfer ions from the drift tube to a unit-mass-resolution quadrupole mass analyzer (Pfeiffer). This instrument is described further by de Gouw and Warneke (2007). The H_3O^+ ToF-CIMS uses RF-only segmented quadrupole ion guides to transfer ions from the drift tube to a time-of-flight mass analyzer with a mass resolution of 4000-6000 produced by Aerodyne Research Inc. / Tofwerk (Bertram et al., 2011). This instrument is described further by Yuan et al. (2016). A similar PTR-ToF instrument using quadrupole ion guides has also been recently described (Sulzer et al., 2014).

Atmos. Meas. Tech. Discuss., doi:10.5194/amt-2016-78, 2016
Manuscript under review for journal Atmos. Meas. Tech.
Published: 7 April 2016

Atmospheric Measurement Techniques Discussions

A gas chromatograph (GC) instrument was used both as an interface to the ToF-CIMS and as a separate instrument using an electron-impact quadrupole mass spectrometer. The GC collects VOCs in a liquid nitrogen cryotrap for a 5 minute period every 30 minutes. VOCs are then injected onto parallel Al_2O_3/KCl PLOT and semi-polar DB-624 capillary columns to separate C2-C11 hydrocarbons and heteroatom-containing VOCs. When used as an interface to the ToF-CIMS, the column eluant was directed to the inlet of the ToF-CIMS, where it was diluted with 50 sccm of dry clean air. When operated as a separate instrument, the column eluant was directed to an electron-ionization quadrupole mass spectrometer (EIMS) operated in selected-ion mode. The response of this GC-EIMS instrument to various VOCs has been well characterized over a long period of field and laboratory applications, and further operational details have been reported elsewhere (Goldan et al., 2004;Gilman et al., 2010;Gilman et al., 2013).

2.2 Adaptation of H_3O^+ to NO^+ CIMS.

Ideally, both H_3O^+ and NO^+ reagent ion chemistry can be utilized with a single instrument. The fewest possible number of hardware parameters were changed to facilitate fast switching and instrument stability.

To achieve generation of NO^+ ions, the water reservoir was replaced with ultra-high purity air. The source gas flow (5 sccm), the hollow cathode parameters, and the drift tube operating pressure (2.4mbar) were not changed. To optimize the generation of NO^+ ions relative to H_3O^+, O_2^+, and NO_2^+, and the generation of the desired VOC^+ ion products, the voltages of the intermediate chamber plates, V_{IC1} and V_{IC2}, and the drift tube voltage V_{DT} were adjusted. An instrument schematic showing the locations of V_{IC1}, V_{IC2}, and V_{DT} can be found in the supplementary information (Fig. S1). Optimization was performed sampling dry air.

It has been demonstrated that the quadrupole ion guides of the ToF-CIMS can significantly change the measured distribution of reagent and impurity ions (Yuan et al., 2016). The PTR-QMS does not have that issue as strongly and therefore we explored the effect of V_{IC1}, V_{IC2}, and V_{DT} on reagent ion distribution using the PTR-QMS. As the PTR-QMS and ToF-CIMS have nearly identical ion source and drift tube design, we assume that ion behavior in these regions is the same for the two instruments.

First, V_{DT} was held constant at 720V (the original setting of the PTR-QMS instrument), and V_{IC1} and V_{IC2} were varied (Fig. 1). The settings of V_{IC1} (140V) and V_{IC2} (80V) were selected

Atmos. Meas. Tech. Discuss., doi:10.5194/amt-2016-78, 2016
Manuscript under review for journal Atmos. Meas. Tech.
Published: 7 April 2016

Atmospheric Measurement Techniques Discussions

as a compromise between high NO^+ ion count rate and low impurity ion count rates. The major impurity ions are H_3O^+, O_2^+, and NO_2^+, and it is desirable to limit the formation of these ions because they react with VOCs, complicating the interpretation of spectra. Next, several VOCs with different functional groups were introduced into the instrument, separately, and the drift tube electric potential scanned. A drift tube voltage of 350 V (electric field intensity relative to gas number density E/N= 60 Td) was selected as a compromise between maximizing NO^+ ion count rate, minimizing H_3O^+, O_2^+, and NO_2^+, maximizing VOC ion count rates, minimizing alkane fragmentation, and promoting different product ions for carbonyls and aldehydes (Fig. 2). This setting results in about 10e6 cps of NO^+ primary ions, while in typical PTR-MS settings we achieve about 30e6 cps of H_3O^+ primary ions.

We note that the E/N of 60 Td used for the NO^+ CIMS is much lower than that used in typical PTRMS settings (circa 120 Td). In air, NO^+ will react with water to produce H_3O^+ and HNO_2 (Fehsenfeld et al., 1971). The electric field in the drift tube limits the formation of the $NO^+\cdot(H_2O)_n$ intermediaries in this reaction, promoting high NO^+ count rates and VOC sensitivity. In PTRMS, the drift field is used to prevent the formation of analogous $H_3O^+\cdot(H_2O)_n$ clusters. The bond energy of $H_3O^+\cdot(H_2O)_n$ clusters is significantly higher than that of $NO^+\cdot(H_2O)_n$ clusters (Keesee and Castleman, 1986), hence the need for a higher E/N in PTRMS settings.

The remainder of the work detailed in this manuscript was performed using the ToF-CIMS with the settings as described here. The ToF-CIMS has the advantages of high mass resolution, fast time resolution, and simultaneous measurement of all masses. Further small adjustments were made to the ToF-CIMS quadrupole ion guide voltages using Thuner software (Tofwerk AG) to promote sensitivity to VOCs and separate carbonyl isomers.

3. Results and Discussion

3.1 Laboratory experiments

3.1.1 Sensitivity and simplicity of the NO^+ reagent ion chemistry

VOCs from several calibration cylinders (VOCs listed in Table S1) were diluted with high purity air to mixing ratios of approximately 10 ppbv, and introduced into the sampling inlet of the GC interface. Eluant from the column was directed into the ToF CIMS as described above. Several species co-elute with another compound (m- and p- xylenes; myrcene and camphene; 1-ethyl,3-

Atmos. Meas. Tech. Discuss., doi:10.5194/amt-2016-78, 2016
Manuscript under review for journal Atmos. Meas. Tech.
Published: 7 April 2016

Atmospheric Measurement Techniques Discussions

methylbenzene and 1-ethyl,4-methylbenzene); reported sensitivities and product ions are an average of the two co-eluting species.

Each VOC mixture was sampled twice, once with H_3O^+ and once with NO^+ reagent ion chemistry and instrument settings. Based on the results we evaluated the utility of NO^+ CIMS relative to H_3O^+ CIMS using two metrics. The first metric is sensitivity for individual VOCs. To determine the sensitivity (*S*), the signals (counts per second) of all product ions were integrated over the width of the chromatographic peak and sensitivities for the measured VOCs using NO^+ chemistry were calculated relative to the sensitivity using H_3O^+ chemistry (S_{NO+}/S_{H3O+}). For several VOCs, we also calculated the relative sensitivity if only the most abundant product ion (the quantitation ion) is measured (Table 2B).

The second metric is the simplicity of spectra. In an ideal instrument, each VOC would produce only one product ion, and each ion mass would be produced by only one VOC. However, using NO^+ and H_3O^+ reagent ions, fragmentation of product ions does occur. As a metric for the complexity of the product ion distribution resulting from particular VOCs, we determined the fraction of the most abundant ion to the total signal from this VOC (*F*) and discuss (F_{NO+}) relative to (F_{H3O+}). Figure S2 contains a comparison of F_{NO+} and F_{H3O+}, and an example product ion distribution. A larger value of this ratio means that NO^+ reagent ion chemistry creates a simpler product ion distribution for that particular VOC. This metric does not indicate whether a particular product ion is produced by only one VOC. Uniqueness of product ions is discussed in Sect. 3.1.2. The NO^+ CIMS product ion distributions of 25 atmospherically relevant VOCs are reported in Table 2.

Figure 3 summarizes the comparison between NO^+ and H_3O^+ reagent ion chemistry for the two metrics. On the y-axis the spectrum simplicity metric and on the x-axis the sensitivity metric are shown.

Branched alkanes and most cyclic alkanes are detected with far greater sensitivity using NO^+ chemical ionization than with H_3O^+ chemical ionization. Aromatics and alkenes are detected slightly more sensitively, and, on average, ketones are detected slightly less sensitively. Alcohols are detected more sensitively, by at least a factor of two, with the exception of methanol. The lower sensitivity to methanol is consistent with slower reaction kinetics reported in the literature (Španěl and Smith, 1997). Monoterpenes and acetonitrile are detected substantially less sensitively.

Atmos. Meas. Tech. Discuss., doi:10.5194/amt-2016-78, 2016
Manuscript under review for journal Atmos. Meas. Tech.
Published: 7 April 2016

Atmospheric Measurement Techniques Discussions

In comparing the simplicity of the product ion distribution between H_3O^+ and NO^+ chemistry, most branched and cyclic alkanes, ketones, and monoterpenes have a higher fraction of signal on a single product ion (simpler spectra). We also highlight that many alkyl substituted aromatics fragment substantially with H_3O^+ chemistry but do not with NO^+ chemistry. The few exceptions (notably, benzene) create more complicated spectra because an NO^+ cluster product is also present (*m+30*).

3.1.2 Distribution of product ions

Product ions of C4-C10 alkenes, aldehydes, ketones, alcohols, and aromatics are consistent with product ion distributions and mechanisms reported from SIFT investigations. Reaction mechanism (charge transfer, hydride transfer, or cluster formation) is dependent on the thermodynamics of charge transfer and hydride transfer (Fig. 4, Table 1, values from Lias et al. (1988)). Charge transfer occurs if the reaction enthalpy is favorable, regardless of the hydride transfer enthalpy. If the charge transfer enthalpy is close to zero, then NO^+ clustering occurs; and if charge transfer is not favorable but hydride transfer is, then hydride transfer will occur. Carbonyls participate in two mechanisms: ketones cluster with NO^+, and aldehydes hydride transfer. Branched alkanes exclusively undergo hydride transfer, and other functional groups participate in other mechanisms: aromatics undergo charge transfer and occasionally cluster; alcohols undergo hydride transfer, and alkenes charge transfer, cluster, or hydride transfer depending on the size of the molecule and the location of the double bond within the molecule.

3.1.3 Alkane fragmentation

Small (C4-C10) branched alkanes cannot be measured by H_3O^+ CIMS. With NO^+ CIMS, these VOCs are detectable but generally fragment to produce several ionic fragments that are common to different species. These masses (for example, m/z 57 $C_4H_9^+$) are produced by many different compounds and are likely not useful for chemically resolved atmospheric measurements. A few masses (e.g. m/z 71 $C_5H_{11}^+$ and m/z 85 $C_6H_{13}^+$) are only produced by a few compounds and were therefore targeted for further investigation in ambient air measurements. Conversely, cyclic alkanes fragment very little. Fig. 5 shows the product ion distributions of several representative aliphatic compounds. We note that the major product ions of cyclic alkanes *(M-H)* are the same with H_3O^+ and with NO^+ chemistry. However, the mechanism is different: NO^+ ionizes by hydride abstraction, while H_3O^+ ionizes by protonation followed by loss of H_2 (Midey et al., 2003). The H_3O^+ ionization mechanism has a secondary channel consisting of protonation followed by

Atmos. Meas. Tech. Discuss., doi:10.5194/amt-2016-78, 2016
Manuscript under review for journal Atmos. Meas. Tech.
Published: 7 April 2016

Atmospheric Measurement Techniques Discussions

elimination of CH_4 or C_nH_{2n} (Midey et al., 2003). The difference in ionization mechanism is a likely explanation for the lower degree of fragmentation observed using NO^+ chemistry.

Compared to small (C8 and smaller) alkanes, large (C12 and higher) n-alkanes show little fragmentation, with at least 50% of the total ion signal accounted for by the expected parent mass (*m-1*) (Fig. 6). Additionally, the degree of fragmentation decreases with increasing carbon chain length. It is quite difficult to measure these compounds with H_3O^+ CIMS because they fragment extensively and are not detected sensitively (Erickson et al., 2014). NO^+ CIMS could provide a fast, sensitive, chemically specific measurement of these compounds. It should be mentioned that large n-alkanes (C10 and larger) are not measureable with the GC interface. Dodecane ($C_{12}H_{26}$), tridecane ($C_{13}H_{28}$), tetradecane ($C_{14}H_{30}$), and pentadecane ($C_{15}H_{32}$) were sampled directly with the NO^+ ToF-CIMS and product ions were identified by correlation with the expected major product ion (*m-1*). The NO^+ ToF-CIMS sensitivity to pentadecane was determined using a permeation source (Veres et al., 2010).

3.1.4 Instrument response factor for select compounds

A calibration factor was determined for various VOCs by (1) direct calibration, (2) estimation from sensitivity relative to H_3O^+ CIMS, or (3) estimation from correlation with GC-EIMS (Table 2). Direct calibrations were performed by mixing a known concentration of a VOC from either a permeation cell (pentadecane) or a calibration gas cylinder (other VOCs) into a dry high-purity air dilution stream. Calibration factors estimated from sensitivity relative to H_3O^+ CIMS were calculated using H_3O^+ ToF-CIMS calibration factors and results from laboratory GC-CIMS experiments (Sect. 3.1.1). Calibration factors for H_3O^+ ToF-CIMS were determined in previous work (Yuan et al., 2016). These calibration factors were multiplied by the relative peak areas determined in Sect. 3.1.1 to obtain estimated NO^+ ToF-CIMS calibration factors. (An example chromatogram and calculation is shown in Fig. S3). Calibration factors estimated from correlation with GC-EIMS were calculated from the slope of NO^+ Tof-CIMS measurements against GC-EIMS measurements in ambient air (discussed in further detail in Sect. 3.2.2).

In the following discussion we use two metrics of instrument response: counts-per-second (cps) and normalized counts-per-second (ncps). Counts-per-second (cps) is the raw ion count rate of the instrument. Two operations were applied to cps measurements to obtain ncps. First, a duty cycle correction (*d.c.c.*) was applied (Chernushevich et al., 2001):

Atmos. Meas. Tech. Discuss., doi:10.5194/amt-2016-78, 2016
Manuscript under review for journal Atmos. Meas. Tech.
Published: 7 April 2016

Atmospheric Measurement Techniques Discussions

$$I_{corr} = cps \times \sqrt{\frac{m/z_{reference}}{m/z}} \quad (1)$$

where I_{corr} is the duty-cycle corrected ion count rate and $m/z_{reference}$ is an arbitrary reference mass (in this work $m/z_{reference} \equiv 55$). The duty-cycle correction accounts for differences in ion residence time in the extraction region of the ToF and eliminates a mass-dependent sensitivity bias. Then, measurements were normalized to the duty-cycle corrected NO^+ (primary ion) measurement, which typically has count rates on the order of 10^6 above that of VOCs:

$$ncps = 10^6 \frac{I_{corr}}{NO^+_{corr}} \quad (2)$$

The normalization removes variability due to fluctuations in the ion source and detector. In calculating limits of detection, we use duty-cycle uncorrected cps, as this best reflects the fundamental counting statistics of the instrument. In reporting ambient air measurements, we use ncps. The ncps measurement reduces several significant instrumental biases and better reflects VOC abundances in air.

Limits of detection at 1Hz measurement frequency were calculated by finding the mixing ratio at which the signal-to-noise ratio (S/N) is equal to 3. The calculation can be expressed by (Bertram et al., 2011;Yuan et al., 2016):

$$\frac{S}{N} = 3 = \frac{C_f[X]_{lod}t}{\alpha \times \sqrt{C_f[X]_{lod}t + 2Bt}} \quad (3)$$

where C_f is the instrument response factor, in cps per ppb; $[X]_{lod}$ is the limit-of-detection mixing ratio of species X in ppb; t is the sampling period of 1 second; α is the scaling factor of noise compared to expected Poissonian counting statistics; and B is the background count rate in cps. The scaling factor α is generally greater than 1 because high-resolution peak overlap and fitting algorithms create additional noise (Cubison and Jimenez, 2015). For comparison, H_3O^+ ToF-CIMS limits of detection, using the same ToF-CIMS instrument, are included where available.

Aliphatics and aromatics are generally detected quite sensitively. Aromatics have sub-100 ppt detection limits and are detected slightly more sensitively with NO^+ CIMS than with H_3O^+ CIMS, with NO^+ detection limits generally about 30% lower. Aliphatic species are detected with quite low detection limits (less than 50 ppt) and with substantially better sensitivity than H_3O^+: the detection limit of methylcyclohexane using NO^+ is a factor of 27 lower than with H_3O^+.

Atmos. Meas. Tech. Discuss., doi:10.5194/amt-2016-78, 2016
Manuscript under review for journal Atmos. Meas. Tech.
Published: 7 April 2016

Atmospheric Measurement Techniques Discussions

Aldehydes and ketones also have detection limits of around 100 ppt or less, with the exception of acetaldehyde (l.o.d. = 355 ppt). The higher detection limit of acetaldehyde is due to a somewhat higher instrumental background and a lower response factor that is consistent with reaction kinetics (Španěl et al., 1997). Methanol has a very high detection limit (28 ppb); this is expected from the anomalously low rate constant of the methanol-NO^+ reaction (Španěl and Smith, 1997). In contrast, ethanol is detected far more sensitively with NO^+ than with H_3O^+, with a detection limit of 105 ppt (compared to 1600 ppt for H_3O^+).

3.1.5 Humidity dependence

Humidity-dependent behaviors of primary ions and selected VOCs (acetaldehyde, acetone, isoprene, 2-butanone, benzene, toluene, o-xylene, and 1,3,5-trimethylbenzene) were determined by diluting a VOC calibration standard into humidified air to reach approximately 10ppb mixing ratio, then sampling directly with the NO^+ ToF-CIMS. Air temperature was 27°C. Product ion and signal dependences on humidity for selected primary ions and VOCs are shown in Fig. 7 (additional species are included in Fig. S4). As relative humidity increases, NO^+ (m/z 30) remains relatively constant, while protonated water and protonated water clusters (especially m/z 37, $H_5O_2^+$) increase. As the abundance of H_3O^+ in the drift tube increases, one might expect to see increased products of VOC reaction with H_3O^+ with a corresponding decrease in NO^+ products. Although an increase of H_3O^+ product is seen for some species (e.g. MEK), it is not universally true. For many species, the major effect is that the NO^+ adduct product increases relative to other NO^+ product ions. This effect is especially intense for isoprene, where the isoprene-NO^+ cluster (m/z 98, $C_5H_8NO^+$) increases by a factor of 10 from 0 to 70% relative humidity. A similar humidity effect, observed during SIFT measurements of alkenes, has been reported previously by Diskin et al. (2002), who attributed the effect to better stabilization of excited intermediary $(NO^+ \cdot R)^*$ ions by H_2O. A full investigation of this effect is beyond the scope of this manuscript. In lieu of a complete theoretical understanding of humidity effects, we suggest that an experimental humidity correction could be applied as in Yuan et al. (2016).

3.2 Measurements of urban air

3.2.1 GC-NO^+ CIMS measurements

Measurement of ambient air using the GC interface allowed us to determine which compounds in ambient air produce which masses. This is the essential link between laboratory measurements of calibration standards, and interpretation of ambient NO^+ ToF-CIMS

Atmos. Meas. Tech. Discuss., doi:10.5194/amt-2016-78, 2016
Manuscript under review for journal Atmos. Meas. Tech.
Published: 7 April 2016

Atmospheric Measurement Techniques Discussions

measurements. Ambient air from outside the laboratory was sampled from Oct. 27, 2015-Oct. 30, 2015 through an inlet three meters above ground level, and directed through 10 meters of ½“ diameter Teflon tubing at a flow rate of 17 slpm (residence time approximately 4 seconds). The GC interface subsampled this stream. Eluant from the column was directed into the NO^+ ToF CIMS as described in Sect. 2.1. The laboratory is in an urban area (Boulder, CO) and the inlet was located near a parking lot and loading dock. Instrument background (including the GC interface) was determined by sampling zero air at the beginning and end of each measurement period. Instrument performance and stability, and retention times of selected compounds, were checked at least once per day by sampling a 56-component hydrocarbon calibration standard.

Figure 8 shows several masses from a typical chromatogram. In this chromatogram, it is clear, for instance, that the majority of signal from m/z 83 ($C_6H_{11}^+$) can be attributed to one compound (methylcyclopentane). On the other hand, m/z 57 ($C_4H_9^+$) is produced from many different compounds with comparable intensities. Aldehydes and ketones appear to be well separated, as expected from the laboratory experiments. Figure 9 summarizes the contributions of different VOCs to several ions (m/z 57, $C_4H_9^+$ and m/z 83 $C_6H_{11}^+$) during the entire measurement period. M/z 57 ($C_4H_9^+$) has contributions from many different VOCs, and the relative proportions are highly variable. Conversely, m/z 83 ($C_6H_{11}^+$) is mostly attributable to methylcyclopentane during the majority of the measurement period. M/z 57 ($C_4H_9^+$) does not provide a useful measurement of alkanes, while m/z 83 ($C_6H_{11}^+$) may possibly provide a useful measurement of methylcyclopentane. Corresponding figures for other masses can be found in the supplemental information (Fig. S5-S7). Table 3 summarizes our assessment of key ions.

3.2.2 NO^+ CIMS vs. GC-EIMS Measurement Comparison

Measurements using the GC interface do not provide any information about the fast time response capability of the NO^+ ToF-CIMS. Additionally, not all compounds detectable by NO^+ CIMS and present in ambient air can be transmitted through the GC interface. Simultaneous GC-EIMS and NO^+ ToF-CIMS measurements were conducted to investigate fast NO^+ measurements, determine if there are any significant interferences to key NO^+ masses, and explore NO^+ CIMS response to VOCs not transmittable through the GC interface. Ion masses that are produced by VOCs not detectable with the GC have higher and more variable signal when measured by the NO^+ ToF-CIMS, compared to the GC-ToF-CIMS.

Atmos. Meas. Tech. Discuss., doi:10.5194/amt-2016-78, 2016
Manuscript under review for journal Atmos. Meas. Tech.
Published: 7 April 2016

Atmospheric Measurement Techniques Discussions

Ambient air was sampled into the laboratory as described in the previous section. The GC-EIMS and the NO^+ ToF-CIMS were run as separate instruments and subsampled the 17 SLPM flow at the same point. Measurements were taken from Nov. 4, 2015 through Nov. 6, 2015. The GC-EIMS instrument was operated on a 30-minute schedule. Instrument background was determined from zeros taken at the beginning and end of the measurement period. The 56-component hydrocarbon calibration standard was sampled once per day. The NO^+ ToF-CIMS measured at 1 Hz frequency. Instrument zeros were taken for a two minute period once every hour. Calibration gas from a 10-component hydrocarbon standard was sampled for two minutes once every three hours. At the end of the measurement period, both instruments were disconnected from the ambient air line and sampled air from inside the laboratory for 1.5 hours (three GC samples), to investigate the NO^+ ToF-CIMS response to air with a VOC composition substantially different from urban air.

For all comparisons between the two instruments, the 1Hz NO^+ ToF-CIMS measurements were averaged over the 5-minute GC-EIMS collection period. The NO^+ ToF-CIMS was re-calibrated using air with ambient humidity for the 10 species listed in Table 2A, and no further humidity correction was applied. Correlations between independent GC and calibrated CIMS measurements generally show high correlation coefficient ($R^2 > 0.9$) and slopes close to 1 (examples in Fig. 10a, b). This demonstrates that an adapted NO^+ CIMS instrument retains sensitive measurement of atmospherically important species such as aromatics that are often targeted using PTRMS and in addition can detect compounds such as iso-pentane, sum of 2- and 3-methylpentanes, methylcyclopentane, and sum of C7 cyclic alkanes (Fig. 10c-f) that are usually not detected with PTR-MS. Slopes for calibrated VOCs, and correlation coefficients (R^2) for all VOCs investigated, are included in Table 3.

To assess the ability of the NO^+ Tof-CIMS to separate ketones and aldehydes, we explore measurements of propanal and acetone. The separate measurement of these two species is a good test case because the two peaks are chromatographically well resolved on the GC-EIMS, there are few isomers of C_3H_6O (of which acetone and propanal are likely the only atmospherically relevant species), and independent measurements of these two species are interesting for scientific reasons: aldehydes are generally much more reactive with OH than their ketone isomers and may have significantly different behavior in the atmosphere (Atkinson and Arey, 2003).

Atmos. Meas. Tech. Discuss., doi:10.5194/amt-2016-78, 2016
Manuscript under review for journal Atmos. Meas. Tech.
Published: 7 April 2016

Atmospheric Measurement Techniques Discussions

A time-series of propanal and acetone is shown in Fig. 11a. The two compounds have clearly different behavior in the atmosphere: there is fast (seconds to minutes), high variability in the acetone measurement that is not seen in the propanal measurement, and the longer term (~hours) variability of acetone and propanal is not the same. The fast, high spikes in acetone may come from local sources such as exhaust from chemistry labs in the building. The acetone comparison between the GC-EIMS and the NO^+ ToF-CIMS has a slope of 1.13, a correlation coefficient R^2 of 0.978 and negligible offset. The comparison between the GC and CIMS propanal measurements has an R^2 of 0.928 (Fig. 11b, c).

Several episodes occurred with elevated high-mass n-alkane masses (m/z 169 $C_{12}H_{25}^+$, dodecane; m/z 183 $C_{13}H_{27}^+$, tridecane; m/z 197 $C_{14}H_{29}^+$, tetradecane; m/z 211 $C_{15}H_{31}^+$, pentadecane). Two examples are shown in Fig. 12. The episodes show high temporal and compositional variability. The inlet was downwind from a parking lot, and next to a loading dock and electric power generator for the building, and it is likely that the elevated C12-C15 alkanes are from any or all of these sources. An ambient air measurement of these species is particularly interesting because they have been implicated in efficient secondary organic aerosol production from diesel fuel exhaust (Gentner et al., 2012).

4. Summary and conclusions

In summary, an H_3O^+ ToF-CIMS (PTR-MS) instrument was easily and inexpensively converted into an NO^+ CIMS by replacing the reagent source gas and modifying the ion source and drift tube voltages. The usefulness of NO^+ CIMS for atmospheric VOC measurement was then evaluated by (1) using a GC interface to determine product ion distributions for nearly 100 VOCs and compare the sensitivity and simplicity of spectra to H_3O^+ CIMS, (2) measuring ambient air with a GC interface, to map product ions to their VOC precursors and determine which ions may be useful for chemically specific measurement, and (3) measuring ambient air directly, to evaluate chemical specificity and investigate fast (1Hz) time measurement of new compounds. Additionally, the NO^+ CIMS response to C12-C15 n-alkanes, and to variable humidity was determined in some detail. Further work is needed to better understand the humidity dependence.

NO^+ CIMS is a valuable technique for atmospheric measurement because it can separate small carbonyl isomers, it can provide fast and chemically specific measurement of cyclic and a few important branched alkanes (notably, isopentane and methylpentanes) that cannot be detected by PTR-MS, it can measure alkyl-substituted aromatics with less fragmentation than H_3O^+ CIMS,

and it can detect larger (C12-C15) alkanes. With NO^+ CIMS significant fragmentation of most small alkanes does occur, making them difficult to measure quantitatively. There are also interferences on many alcohols (with the exception of ethanol) and butanal. Additionally, it is worth considering that $VOC{\cdot}NO^+$ cluster formation moves certain species into a higher mass range. This may be a drawback because the number of possible isobaric compounds increases with mass, and it may be more difficult for high-resolution peak-fitting algorithms to separate species of interest from isobaric interferences (example in Fig. S8). Finally, because there are three different ionization mechanisms, (hydride transfer, charge transfer, and NO^+ adduct formation), it may be difficult to determine which VOC precursors correspond to particular ions. NO^+ CIMS may be an extremely useful supplementary approach for specific applications such as studying secondary organic aerosol precursors in vehicle exhaust, investigating emissions from oil and natural gas extraction, identifying additional species in complex emissions such as biomass burning, measuring emissions of oxygenated consumer products and solvents in urban areas, and investigating photochemistry of biogenic VOCs.

Author Contribution

P. Veres and C. Warneke obtained project funding. B. Yuan, A. Koss, C. Warneke, and J. de Gouw developed the ToF-CIMS instrument. A. Koss converted the instrument from H_3O^+ to NO^+, designed the experiments, collected data, and wrote the manuscript. A. Koss and M. Coggon analyzed data. C. Warneke and J. de Gouw provided guidance on experimental design and interpretation. All authors edited the manuscript.

Acknowledgements

This work was funded by the CIRES Innovative Research Program. A. R. Koss acknowledges additional support from the NSF Graduate Fellowship Program. We would like to thank J. B. Gilman and B. M. Lerner for help with GC operation and data analysis.

References

Agarwal, B., González-Méndez, R., Lanza, M., Sulzer, P., Märk, T. D., Thomas, N., and Mayhew, C. A.: Sensitivity and Selectivity of Switchable Reagent Ion Soft Chemical Ionization Mass Spectrometry for the Detection of Picric Acid, J. Phys. Chem. A, 118, 8229-8236, 10.1021/jp5010192, 2014.

Arnold, S. T., Viggiano, A. A., and Morris, R. A.: Rate Constants and Product Branching Fractions for the Reactions of H3O+ and NO+ with C2−C12 Alkanes, J. Phys. Chem. A, 102, 8881-8887, 10.1021/jp9815457, 1998.

448 Atkinson, R., and Arey, J.: Atmospheric degradation of volatile organic compounds, Chem. Rev., 103,
449 4605-4638, 2003.
450 Bertram, T. H., Kimmel, J. R., Crisp, T. A., Ryder, O. S., Yatavelli, R. L. N., Thornton, J. A., Cubison, M. J.,
451 Gonin, M., and Worsnop, D. R.: A field-deployable, chemical ionization time-of-flight mass
452 spectrometer, Atmos. Meas. Tech., 4, 1471-1479, 10.5194/amt-4-1471-2011, 2011.
453 Buhr, K., van Ruth, S., and Delahunty, C.: Analysis of volatile flavour compounds by Proton Transfer
454 Reaction-Mass Spectrometry: fragmentation patterns and discrimination between isobaric and
455 isomeric compounds, Int. J. Mass Spectrom., 221, 1-7, http://dx.doi.org/10.1016/S1387-
456 3806(02)00896-5, 2002.
457 Chernushevich, I. V., Loboda, A. V., and Thomson, B. A.: An introduction to quadrupole–time-of-flight
458 mass spectrometry, J. Mass Spectrom., 36, 849-865, 10.1002/jms.207, 2001.
459 Cubison, M. J., and Jimenez, J. L.: Statistical precision of the intensities retrieved from constrained fitting
460 of overlapping peaks in high-resolution mass spectra, Atmos. Meas. Tech., 8, 2333-2345, 10.5194/amt-
461 8-2333-2015, 2015.
462 de Gouw, J., and Warneke, C.: Measurements of volatile organic compounds in the earth's atmosphere
463 using proton-transfer-reaction mass spectrometry, Mass. Spectrom. Rev., 26, 223-257,
464 10.1002/mas.20119, 2007.
465 Diskin, A. M., Wang, T., Smith, D., and Španěl, P.: A selected ion flow tube (SIFT), study of the reactions
466 of H3O+, NO+ and O2+ ions with a series of alkenes; in support of SIFT-MS, Int. J. Mass Spectrom., 218,
467 87-101, http://dx.doi.org/10.1016/S1387-3806(02)00662-0, 2002.
468 Erickson, M. H., Gueneron, M., and Jobson, B. T.: Measuring long chain alkanes in diesel engine exhaust
469 by thermal desorption PTR-MS, Atmos. Meas. Tech., 7, 225-239, 10.5194/amt-7-225-2014, 2014.
470 Fehsenfeld, F. C., Mosesman, M., and Ferguson, E. E.: Ion—Molecule Reactions in NO+–H2O System, J.
471 Chem. Phys., 55, 2120-2125, doi:http://dx.doi.org/10.1063/1.1676383, 1971.
472 Francis, G. J., Milligan, D. B., and McEwan, M. J.: Gas-Phase Reactions and Rearrangements of Alkyl
473 Esters with H3O+, NO+, and O2•+: A Selected Ion Flow Tube Study, J. Phys. Chem. A, 111, 9670-9679,
474 10.1021/jp0731304, 2007a.
475 Francis, G. J., Wilson, P. F., Milligan, D. B., Langford, V. S., and McEwan, M. J.: GeoVOC: A SIFT-MS
476 method for the analysis of small linear hydrocarbons of relevance to oil exploration, Int. J. Mass
477 Spectrom., 268, 38-46, 10.1016/j.ijms.2007.08.005, 2007b.
478 Gentner, D. R., Isaacman, G., Worton, D. R., Chan, A. W. H., Dallmann, T. R., Davis, L., Liu, S., Day, D. A.,
479 Russell, L. M., Wilson, K. R., Weber, R., Guha, A., Harley, R. A., and Goldstein, A. H.: Elucidating
480 secondary organic aerosol from diesel and gasoline vehicles through detailed characterization of
481 organic carbon emissions, Proc. Natl. Acad. Sci. USA, 109, 18318-18323, 10.1073/pnas.1212272109,
482 2012.
483 Gilman, J. B., Burkhart, J. F., Lerner, B. M., Williams, E. J., Kuster, W. C., Goldan, P. D., Murphy, P. C.,
484 Warneke, C., Fowler, C., Montzka, S. A., Miller, B. R., Miller, L., Oltmans, S. J., Ryerson, T. B., Cooper, O.
485 R., Stohl, A., and de Gouw, J. A.: Ozone variability and halogen oxidation within the Arctic and sub-
486 Arctic springtime boundary layer, Atmos. Chem. Phys., 10, 10223-10236, 10.5194/acp-10-10223-2010,
487 2010.
488 Gilman, J. B., Lerner, B. M., Kuster, W. C., and de Gouw, J. A.: Source signature of volatile organic
489 compounds from oil and natural gas operations in northeastern Colorado, Environ. Sci. Technol., 47,
490 1297-1305, 10.1021/es304119a, 2013.
491 Glasius, M., and Goldstein, A. H.: Recent Discoveries and Future Challenges in Atmospheric Organic
492 Chemistry, Environ. Sci. Technol., 10.1021/acs.est.5b05105, 2016.
493 Goldan, P. D., Kuster, W. C., Williams, E., Murphy, P. C., Fehsenfeld, F. C., and Meagher, J.: Nonmethane
494 hydrocarbon and oxy hydrocarbon measurements during the 2002 New England Air Quality Study, J.
495 Geophys. Res.: Atmos., 109, 2156-2202, doi:10.1029/2003JD004455, 2004.

496 Graus, M., Müller, M., and Hansel, A.: High Resolution PTR-TOF: Quantification and Formula
497 Confirmation of VOC in Real Time, J. Am. Soc. Mass Spectr., 21, 1037-1044,
498 http://dx.doi.org/10.1016/j.jasms.2010.02.006, 2010.
499 Gueneron, M., Erickson, M. H., VanderSchelden, G. S., and Jobson, B. T.: PTR-MS fragmentation patterns
500 of gasoline hydrocarbons, Int. J. Mass Spectrom., 379, 97-109,
501 http://dx.doi.org/10.1016/j.ijms.2015.01.001, 2015.
502 Inomata, S., Tanimoto, H., and Yamada, H.: Mass Spectrometric Detection of Alkanes Using NO+
503 Chemical Ionization in Proton-transfer-reaction Plus Switchable Reagent Ion Mass Spectrometry,
504 Chem. Lett., 43, 538-540, 10.1246/cl.131105, 2013.
505 Jobson, B. T., Alexander, M. L., Maupin, G. D., and Muntean, G. G.: On-line analysis of organic
506 compounds in diesel exhaust using a proton transfer reaction mass spectrometer (PTR-MS), Int. J.
507 Mass Spectrom., 245, 78-89, http://dx.doi.org/10.1016/j.ijms.2005.05.009, 2005.
508 Jordan, A., Haidacher, S., Hanel, G., Hartungen, E., Herbig, J., Märk, L., Schottkowsky, R., Seehauser, H.,
509 Sulzer, P., and Märk, T. D.: An online ultra-high sensitivity Proton-transfer-reaction mass-spectrometer
510 combined with switchable reagent ion capability (PTR + SRI − MS), Int. J. Mass Spectrom., 286, 32-38,
511 http://dx.doi.org/10.1016/j.ijms.2009.06.006, 2009a.
512 Jordan, A., Haidacher, S., Hanel, G., Hartungen, E., Märk, L., Seehauser, H., Schottkowsky, R., Sulzer, P.,
513 and Märk, T. D.: A high resolution and high sensitivity proton-transfer-reaction time-of-flight mass
514 spectrometer (PTR-TOF-MS), Int. J. Mass Spectrom., 286, 122-128,
515 http://dx.doi.org/10.1016/j.ijms.2009.07.005, 2009b.
516 Karl, T., Hansel, A., Cappellin, L., Kaser, L., Herdlinger-Blatt, I., and Jud, W.: Selective measurements of
517 isoprene and 2-methyl-3-buten-2-ol based on NO+ ionization mass spectrometry, Atmos. Chem. Phys.,
518 12, 11877-11884, 10.5194/acp-12-11877-2012, 2012.
519 Katzenstein, A. S., Doezema, L. A., Simpson, I. J., Blake, D. R., and Rowland, F. S.: Extensive regional
520 atmospheric hydrocarbon pollution in the southwestern United States, P. Natl. Acad. Sci. USA, 100,
521 11975-11979, 10.1073/pnas.1635258100, 2003.
522 Keesee, R. G., and Castleman, A. W.: Thermochemical Data on Gas-Phase Ion-Molecule Association and
523 Clustering Reactions, J. Phys. Chem. Ref. Data, 15, 1011, 10.1063/1.555757, 1986.
524 Knighton, W. B., Fortner, E. C., Herndon, S. C., Wood, E. C., and Miake-Lye, R. C.: Adaptation of a proton
525 transfer reaction mass spectrometer instrument to employ NO+ as reagent ion for the detection of
526 1,3-butadiene in the ambient atmosphere, Rapid Commun. Mass Sp., 23, 3301-3308,
527 10.1002/rcm.4249, 2009.
528 Lias, S. G., Bartmess, J. E., Liebman, J. F., Holmes, J. L., Levin, R. D., and Mallard, W. G.: Gas-Phase Ion
529 and Neutral Thermochemistry, J. Phys. Chem. Ref. Data, 17, 1988.
530 Liu, Y. J., Herdlinger-Blatt, I., McKinney, K. A., and Martin, S. T.: Production of methyl vinyl ketone and
531 methacrolein via the hydroperoxyl pathway of isoprene oxidation, Atmos. Chem. Phys., 13, 5715-
532 5730, 10.5194/acp-13-5715-2013, 2013.
533 Midey, A. J., Williams, S., Miller, T. M., and Viggiano, A. A.: Reactions of O2+, NO+ and H3O+ with
534 methylcyclohexane (C7H14) and cyclooctane (C8H16) from 298 to 700 K, Int. J. Mass Spectrom., 222,
535 413-430, http://dx.doi.org/10.1016/S1387-3806(02)00996-X, 2003.
536 Prince, B. J., Milligan, D. B., and McEwan, M. J.: Application of selected ion flow tube mass spectrometry
537 to real-time atmospheric monitoring, Rapid Commun. Mass Sp., 24, 1763-1769, 10.1002/rcm.4574,
538 2010.
539 Smith, D., and Španěl, P.: Selected ion flow tube mass spectrometry (SIFT-MS) for on-line trace gas
540 analysis, Mass Spectrom. Rev., 24, 661-700, 10.1002/mas.20033, 2005.
541 Španěl, P., and Smith, D.: A selected ion flow tube study of the reactions of NO+ and O+2 ions with some
542 organic molecules: The potential for trace gas analysis of air, J. Chem. Phys., 104, 1893-1899,
543 doi:http://dx.doi.org/10.1063/1.470945, 1996.

544 Španěl, P., Ji, Y., and Smith, D.: SIFT studies of the reactions of H3O+, NO+ and O2+ with a series of
545 aldehydes and ketones, Int. J. Mass Spectrom., 165–166, 25-37, http://dx.doi.org/10.1016/S0168-
546 1176(97)00166-3, 1997.
547 Španěl, P., and Smith, D.: SIFT studies of the reactions of H3O+, NO+ and O2+ with a series of alcohols,
548 Int. J. Mass Spectrom., 167–168, 375-388, http://dx.doi.org/10.1016/S0168-1176(97)00085-2, 1997.
549 Španěl, P., and Smith, D.: Selected ion flow tube studies of the reactions of H3O+, NO+, and O2+ with
550 several aromatic and aliphatic hydrocarbons, Int. J. Mass Spectrom., 181, 1-10,
551 http://dx.doi.org/10.1016/S1387-3806(98)14114-3, 1998a.
552 Španěl, P., and Smith, D.: Selected ion flow tube studies of the reactions of H3O+, NO+, and O2+ with
553 several amines and some other nitrogen-containing molecules, Int. J. Mass Spectrom., 176, 203-211,
554 http://dx.doi.org/10.1016/S1387-3806(98)14031-9, 1998b.
555 Španěl, P., and Smith, D.: Selected ion flow tube studies of the reactions of H3O+, NO+, and O2+ with
556 several aromatic and aliphatic monosubstituted halocarbons, Int. J. Mass Spectrom., 189, 213-223,
557 http://dx.doi.org/10.1016/S1387-3806(99)00103-7, 1999.
558 Sulzer, P., Hartungen, E., Hanel, G., Feil, S., Winkler, K., Mutschlechner, P., Haidacher, S., Schottkowsky,
559 R., Gunsch, D., Seehauser, H., Striednig, M., Jürschik, S., Breiev, K., Lanza, M., Herbig, J., Märk, L.,
560 Märk, T. D., and Jordan, A.: A Proton Transfer Reaction-Quadrupole interface Time-Of-Flight Mass
561 Spectrometer (PTR-QiTOF): High speed due to extreme sensitivity, Int. J. Mass Spectrom., 368, 1-5,
562 http://dx.doi.org/10.1016/j.ijms.2014.05.004, 2014.
563 Veres, P., Gilman, J. B., Roberts, J. M., Kuster, W. C., Warneke, C., Burling, I. R., and de Gouw, J.:
564 Development and validation of a portable gas phase standard generation and calibration system for
565 volatile organic compounds, Atmos. Meas. Tech., 3, 683-691, 10.5194/amt-3-683-2010, 2010.
566 Warneke, C., de Gouw, J. A., Lovejoy, E. R., Murphy, P. C., Kuster, W. C., and Fall, R.: Development of
567 Proton-Transfer Ion Trap-Mass Spectrometry: On-line Detection and Identification of Volatile Organic
568 Compounds in Air, J. Am. Soc. Mass Spectrom., 16, 1316-1324,
569 http://dx.doi.org/10.1016/j.jasms.2005.03.025, 2005.
570 Yuan, B., Koss, A., Warneke, C., Gilman, J. B., Lerner, B. M., Stark, H., and de Gouw, J. A.: A high-
571 resolution time-of-flight chemical ionization mass spectrometer utilizing hydronium ions (H3O+ ToF-
572 CIMS) for measurements of volatile organic compounds in the atmosphere, Atmos. Meas. Tech.
573 Discuss., 2016, 1-43, 10.5194/amt-2016-21, 2016.
574

Atmos. Meas. Tech. Discuss., doi:10.5194/amt-2016-78, 2016
Manuscript under review for journal Atmos. Meas. Tech.
Published: 7 April 2016

Atmospheric Measurement Techniques Discussions

Tables.

Table 1. VOC species in Fig. 4 and their charge transfer and hydride transfer reaction enthalpies.

ID #	Species name	Hydride transfer enthalpy (kJ/mol)	Charge transfer enthalpy (kJ/mol)
0	methanol	22.98	152.05
1	ethene	174.58	120.59
2	acetaldehyde	-61.32	93.20
3	ethane	100.98	217.65
4	ethanol	-68.02	117.31
5	propene	40.17	44.96
6	propanal	-105.32	67.15
7	propane	8.88	161.69
8	n-propanol	-78.72	92.23
9	i-propanol	-122.22	87.41
10	methacrolein	-87.62	63.29
11	1-butene	-39.39	27.59
12	iso-butene	15.88	-4.24
13	2-butenes	17.18	-15.82
14	butanal	-84.02	53.64
15	n-butane	6.98	122.14
16	iso-butane	-56.32	136.61
17	1-butanol	-87.02	70.04
18	2-methylpropanol	-94.02	72.94
19	2-butanol	-137.02	59.43
20	1,4-pentadiene	-69.32	34.35
21	1-pentene	-53.02	21.80
22	2-pentene	-92.02	-23.54
23	3-methyl-1-butene	-92.52	24.70
24	cyclopentane	-7.22	102.84
25	n-pentane	-6.02	98.02
26	iso-pentane	-70.02	101.88
27	neo-pentane	77.98	99.95
28	1-pentanol	-94.02	97.05
29	3-methyl-2-butanol	-143.02	51.71
30	3-pentanol	-140.02	47.85
31	benzene	159.08	-1.93
32	cyclohexane	-28.02	59.43
33	methylcyclopentane	-80.02	42.06
34	4-methyl-2-pentene	-117.82	-27.40
35	3-methyl-1-pentene	-125.22	16.98
36	2,3,-dimethyl-1-butene	-94.02	-18.72
37	n-hexane	-13.92	83.55
38	2-methylpentane	-74.72	72.94
39	2,3-dimethylbutane	-79.22	66.18
40	3-methylpentane	-75.42	69.08
41	toluene	-36.02	-42.06
42	methylcyclohexane	-73.02	36.27
43	1,2-dimethyl-cyclopentane	-95.52	63.29
44	ethylbenzene	-103.02	-47.66
45	o-xylene	-55.02	-67.92
46	m-xylene	-47.22	-68.88
47	p-xylene	-65.92	-79.50
48	isopropylbenzene	-111.92	-51.52
49	3-ethyltoluene	-103.12	-82.41
50	acetone		43.03
51	butanone		24.70
52	2-pentanone		11.19
53	3-pentanone		4.44
54	MVK		37.24

Atmos. Meas. Tech. Discuss., doi:10.5194/amt-2016-78, 2016
Manuscript under review for journal Atmos. Meas. Tech.
Published: 7 April 2016

Atmospheric Measurement Techniques Discussions

Table 2. Sensitivities and detection limits of NO^+ ToF-CIMS for various VOCs. Additional product ions are listed in gray text.

A. Species calibrated directly with NO^+ CIMS

VOC species	Ion formula (% of total signal)				Background cps	Noise scale factor α	NO^+ sensitivity		NO^+ 1-s detection limit	H_3O^+ CIMS 1s detection limit
	Formula	Mechanism	(% of total signal)	Exact m/z (Th)			ncps/ppb	cps/ppb		
Methanol	CH_4ONO^+	M+NO^+	(12%)	62.024	0.88	1.23	0.15	0.45	28 *ppb*	0.397 *ppb*
	CH_4OH^{+*}	M+H^+	(49%)	33.034						
	$CH_7O_2^{+*}$	M+H_3O^+	(39%)	51.044						
Acetonitrile	$C_2H_3NNO^+$	M+NO^+	(48%)	71.024	1.5	1.33	7	30	503 *ppt*	45 *ppt*
	$C_2H_3NH^{+*}$	M+H^+	(44%)	42.034						
	$C_2H_6NO^{+*}$	M+H_3O^+	(8%)	60.044						
Acetaldehyde	$C_2H_3O^+$	M-H^-	(60%)	43.018	46	1.33	41	133	337 *ppt*	195 *ppt*
	$C_2H_5O_2^+$	M-H+H_2O	(13%)	61.028						
	$C_2H_4OH^{+*}$	M+H^+	(11%)	45.034						
	$C_2H_4ONO^+$	M+NO^+	(9%)	74.024						
Acetone	$C_3H_6ONO^+$	M+NO^+	(82%)	88.039	28	1.16	86	394	80 *ppt*	97 *ppt*
	$C_3H_6OH^{+*}$	M+H^+	(13%)	59.049						
Isoprene	$C_5H_8^+$	M^+	(46%)	68.062	0.93	1.34	59	242	58 *ppt*	162 *ppt*
	$C_5H_8NO^+$	M+NO^+	(17%)	98.060						
	$C_5H_7^+$	M-H^-	(7%)	67.054						
MEK	$C_4H_8ONO^+$	M+NO^+	(86%)	102.055	4.1	1.33	157	781	24 *ppt*	45 *ppt*
	$C_4H_8OH^{+*}$	M+H^+	(8%)	73.065						
Benzene†	$C_6H_6^+$	M^+	(55%)	78.046	11	1.37	68	302	88 *ppt*	
	$C_6H_6NO^+$	M+NO^+	(40%)	108.044	10	1.72	50	254	123 *ppt*	96 *ppt*
	sum				*21*	*1.59*	*116*	*556*	*69 ppt*	
Toluene	$C_7H_8^+$	M^+	(89%)	92.062	19	1.33	138	663	*47 ppt*	47 *ppt*
	$C_7H_8NO^+$	M+NO^+	(8%)	122.060						
o-Xylene	$C_8H_{10}^+$	M^+	(94%)	106.078	4.2	1.51	154	789	28 *ppt*	40 *ppt*
	$C_8H_{10}NO^+$	M+NO^+	(5%)	136.076						
1,2,4-Trimethylbenzene	$C_9H_{12}^+$	M^+	(100%)	120.093	1.3	1.75	162	882	22 *ppt*	45 *ppt*
n-Pentadecane	$C_{15}H_{31}^+$	M-H^-	(72%)	211.242	2.7	1.83	48	512	46 *ppt*	---
	$C_9H_{19}^+$	fragment	(3%)	127.148						
	$C_{10}H_{21}^+$	fragment	(3%)	141.164						
	$C_8H_{17}^+$	fragment	(3%)	113.132						

B. Sensitivity estimated via sensitivity relative to H_3O^+ CIMS

VOC species	H_3O^+ cps/ppb	Product ions				Relative (NO^+cps/H_3O^+cps)	Background cps	Noise scale factor α	NO^+ sensitivity		NO^+ 1s detection limit	H_3O^+ CIMS 1s detection limit
		Formula	Mechanism	(% of total signal)	Exact m/z (Th)				ncps/ppb	cps/ppb		
Ethanol	119	$C_2H_5O^+$	M-H^-	(80%)	45.033	6.2	149	1.37	127	738	105 *ppt*	1627 *ppt*
		$C_2H_7O_2^+$	M-H+H_2O	(15%)	63.044							
	27	$C_7H_{13}^+$	M-H^-	(98%)	97.101	17	6.6	1.32	53	448	50 *ppt*	943 *ppt*

Atmos. Meas. Tech. Discuss., doi:10.5194/amt-2016-78, 2016
Manuscript under review for journal Atmos. Meas. Tech.
Published: 7 April 2016

Atmospheric Measurement Techniques Discussions

Methyl-cyclohexane		$C_6H_{11}^+$	fragment	(2%)	83.086							
MVK	539	$C_4H_6ONO^+$	$M+NO^+$	(100%)	100.039	0.38	4	1.71	24	202	112 *ppt*	85 *ppt*
Pentanones	770	$C_5H_{10}ONO^+$	$M+NO^+$	(83%)	116.071	1.18	4.4	1.32	97	906	21 *ppt*	47 *ppt*
		$C_5H_{10}OH^+$*	$M+H^+$	(7%)	87.080							
α-Pinene	262	$C_{10}H_{16}^+$	M^+	(59%)	136.125	0.28	0.39	1.69	7.3	73	233 *ppt*	67 *ppt*
		$C_7H_8^+$	fragment	(24%)	92.062							
		$C_7H_9^+$	fragment	(11%)	93.070							
		$C_{10}H_{16}H^+$*	$M+H^+$	(7%)	137.132							

C. Sensitivity estimated via correlation with GC-EIMS

	Product ions					Back-ground	Noise scale	NO^+ Sensitivity		NO^+ 1-s detection
VOC species	**Formula**	**Mechanism**	**(% of total signal)**	**Exact m/z (Th)**	**Correlation with GC (R^2)**	**cps**	**factor α**	ncps/ppb	cps/ppb	**limit**
Propanal	$C_3H_5O^+$	$M-H^-$	(65%)	57.033	0.928	11	1.40	170	1057	26 *ppt*
	$C_3H_7O_2^+$*	$M-H+H_2O$	(17%)	75.044						
	$C_3H_6OH^+$*	$M+H^+$	(7%)	59.049						
Methacrolein + crotonaldehyde	$C_4H_5O^+$	$M-H^-$	(64%)	69.033	0.984	4.1	1.37	48	325	60 *ppt*
	$C_4H_6ONO^+$	$M+NO^+$	(16%)	100.039						
	$C_3H_5^+$	fragment	(10%)	41.039						
iso-Pentane	$C_5H_{11}^+$	$M-H^-$	(82%)	71.086	0.888	23	1.36	101	706	49 *ppt*
	$C_3H_7^+$	fragment	(11%)	43.054						
Methylcyclopentane	$C_6H_{11}^+$	$M-H^-$	(99%)	83.086	0.961	7.4	1.34	154	1225	18 *ppt*
C5 aldehydes	$C_5H_9O^+$	$M-H^-$	(49%)	85.065	0.936	9.8	1.38	119	904	28 *ppt*
	$C_4H_9^+$	fragment	(22%)	57.070						
	$C_5H_{11}O_2^+$*	$M-H+H_2O$	(19%)	103.075						
2- and 3-methylpentane	$C_6H_{13}^+$	$M-H^-$	(82%)	85.101	0.978	16	1.34	122	981	30 *ppt*
	$C_3H_7^+$	fragment	(10%)	43.054						
	$C_4H_9^+$	fragment	(4%)	57.070						
Hexanal	$C_6H_{11}O^+$	$M-H^-$	(49%)	99.080	0.945	10	1.47	160	1270	22 *ppt*
	$C_6H_{13}O_2^+$*	$M-H+H_2O$	(23%)	117.091						
	$C_5H_{11}^+$	fragment	(15%)	71.086						
Styrene	$C_8H_8^+$	M^+	(100%)	104.062	0.949	0.62	1.47	112	966	15 *ppt*
Benzaldehyde	$C_7H_5O^+$	$M-H^-$	(100%)	105.033	0.923	12	1.37	75	621	43 *ppt*

* Product from residual H_3O^+

† Both product ions can be unambiguously assigned to benzene. We therefore report also the counting statistics and limit of detection for the sum of the two ions.

Atmos. Meas. Tech. Discuss., doi:10.5194/amt-2016-78, 2016
Manuscript under review for journal Atmos. Meas. Tech.
Published: 7 April 2016

Atmospheric Measurement Techniques Discussions

Table 3. Assessment of significant product ions investigated by GC-NO^+ CIMS and parallel GC-EIMS and NO^+ CIMS measurement of ambient air. Masses in bold can be unambiguously assigned to a single VOC or a structurally related, correlated group of VOCs.

Ion formula	Exact mass (Th)	Assessment from series GC-NO^+ ToF-CIMS	Correlation with parallel GC-EIMS R^2	Slope (ppbv/ppbv)
$C_3H_5^+$	41.039	several non-correlated species		
$C_2H_3O^+$	43.018	**acetaldehyde**	**0.942**	**0.892**
$C_3H_7^+$	43.054	several non-correlated species		
$C_2H_5O^+$	45.033	**ethanol**	**0.998**	
$C_4H_6^+$	**54.046**	**propyne**[1]		
$C_4H_8^+$	56.062	several non-correlated species		
$C_3H_5O^+$	57.033	**propanal**	**0.928**	
$C_4H_9^+$	57.070	several non-correlated species		
$C_3H_7O^+$	59.049	interference from acetone; if accounted for, sum of C3 alcohols		
$CH_4NO_2^+$	**62.024**	**methanol, but poor sensitivity**	**0.904**	**1.25**
$C_5H_6^+$	66.046	interference from benzene; if accounted for, cyclopentadiene		
$C_4H_4O^+$	**68.026**	**furan**[2]		
$C_5H_8^+$	68.062	possibly: isoprene[3]		
$C_4H_5O^+$	**69.033**	**methacrolein + crotonaldehyde**[4]	**0.984**	
$C_5H_9^+$	69.070	several non-correlated species		
$C_5H_{10}^+$	70.078	possibly: sum of 2-pentenes[3]		
$C_4H_7O^+$	71.049	several non-correlated species		
$C_5H_{11}^+$	**71.086**	**iso-pentane**	**0.888**	
$C_4H_9O^+$	73.065	several non-correlated species		
$C_6H_6^+$	**78.046**	**benzene**[5]	**0.987**	**0.847**
$C_5H_6O^+$	82.041	possibly: sum of 2- and 3-methylfuran[3]		
$C_6H_{11}^+$	**83.086**	**methylcyclopentane**	**0.961**	
$C_5H_9O^+$	**85.065**	**sum of C5 aldehydes**	**0.936**	
$C_6H_{13}^+$	**85.101**	**sum of 2- and 3-methylpentane**	**0.978**	
$C_4H_8NO^+$	86.060	several non-correlated species		
$C_5H_{11}O^+$	87.080	C5 alcohols and ethers; significant interference from minor carbonyl product ions		
$C_3H_6NO_2^+$	**88.039**	**acetone**	**0.978**	**1.13**
$C_2H_4NO_3^+$	90.019	possibly: acetic acid (chromatography too poor to determine)		
$C_7H_8^+$	**92.062**	**toluene**	**0.999**	**0.810**
$C_7H_{13}^+$	**97.101**	**sum of C7 cyclic alkanes**	**0.917**	
$C_6H_{11}O^+$	**99.080**	**hexanal**	**0.945**	
$C_7H_{15}^+$	99.117	possibly: sum of 2- and 3-methylhexane, but poor sensitivity		
$C_4H_6NO_2^+$	**100.039**	**MVK**	**0.950**	
$C_5H_{10}NO^+$	100.076	possibly: sum of C5 terminal alkenes, but poor sensitivity		
$C_4H_8NO_2^+$	**102.055**	**MEK**	**0.971**	**0.843**
$C_8H_8^+$	**104.062**	**styrene (vinyl benzene)**	**0.949**	
$C_7H_5O^+$	**105.033**	**benzaldehyde**	**0.923**	
$C_8H_{10}^+$	**106.078**	**sum of C8 aromatics**	**0.952**	**0.746**
$C_6H_6NO^+$	**108.044**	**benzene**[5]		
$C_8H_{15}^+$	111.117	possibly: sum of C2 alkyl-substituted cyclohexanes[6]	0.761	
$C_7H_{13}O^+$	**113.096**	**heptanal**[2]		
$C_8H_{17}^+$	113.132	possibly: sum of methylheptanes, but poor sensitivity		
$C_5H_{10}NO_2^+$	**116.071**	**sum of C5 ketones**	**0.945**	
$C_9H_{10}^+$	118.078	possibly: sum of methylstyrene isomers[3]		
$C_9H_{12}^+$	120.093	sum of C9 aromatics; scatter possibly due to disparity in response factors	0.600	
$C_8H_{15}O^+$	**127.112**	**octanal**[2]		

Atmos. Meas. Tech. Discuss., doi:10.5194/amt-2016-78, 2016
Manuscript under review for journal Atmos. Meas. Tech.
Published: 7 April 2016

Atmospheric Measurement Techniques Discussions

$C_6H_{12}NO_2^+$	130.086	possibly: sum of C6 ketones[3]	
$C_{10}H_{14}^+$	134.109	possibly: sum of C10 aromatics	
$C_{10}H_{16}^+$	136.125	monoterpenes plus unknown interference; possibly adamantane from vehicle exhaust	0.584
$C_7H_{14}NO_2^+$	144.102	heptanone[2]	

[1] Cross-comparison with independent GC-EIMS not possible due to chromatographic quantitation ion overlap with neighboring peaks.
[2] Cross-comparison with independent GC-EIMS not possible due to EIMS quadrupole SIS (selected ion scan) window restrictions.
[3] Concentrations too low in ambient air to determine.
[4] Winter urban air sampled was likely influenced by local domestic biomass burning; crotonaldehyde may be a smaller fraction of signal in other environments.
[5] Benzene correlation using sum of m108 $C_6H_6NO^+$ and m78 $C_6H_6^+$.
[6] With exclusion of single outlier, $R^2 = 0.831$.

Atmos. Meas. Tech. Discuss., doi:10.5194/amt-2016-78, 2016
Manuscript under review for journal Atmos. Meas. Tech.
Published: 7 April 2016

Atmospheric Measurement Techniques Discussions

Figures

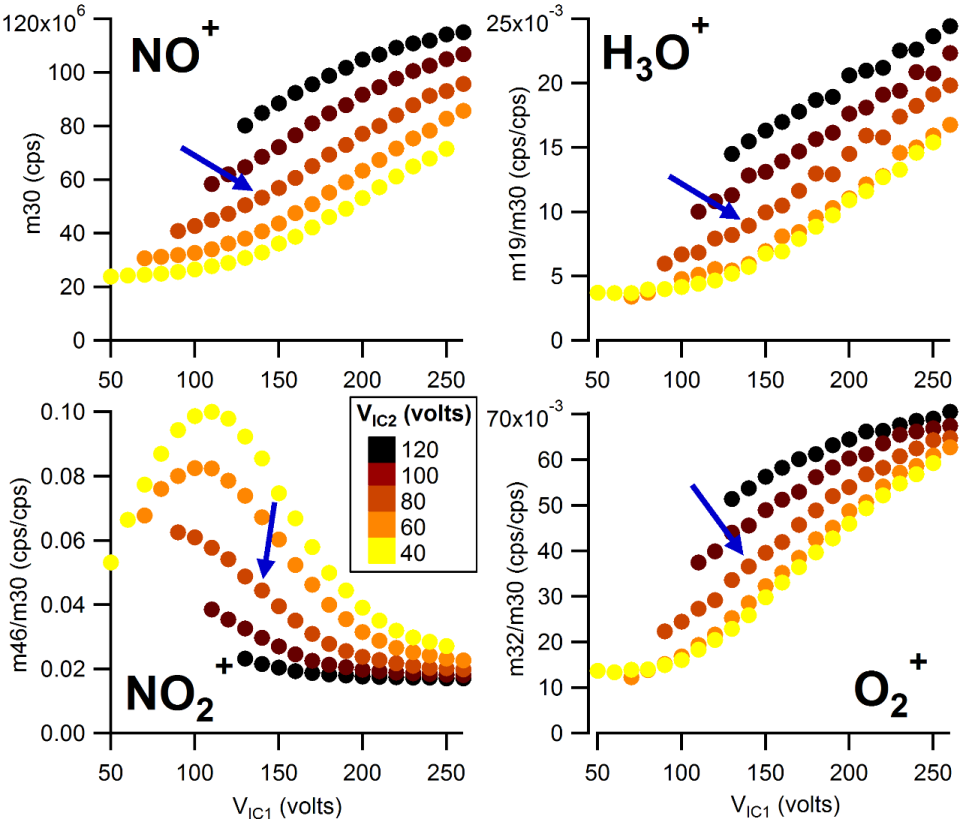

Figure 1. Dependence of NO^+, H_3O^+, NO_2^+, and O_2^+ on intermediate chamber voltages. The arrow denotes the selected operating conditions.

Atmos. Meas. Tech. Discuss., doi:10.5194/amt-2016-78, 2016
Manuscript under review for journal Atmos. Meas. Tech.
Published: 7 April 2016

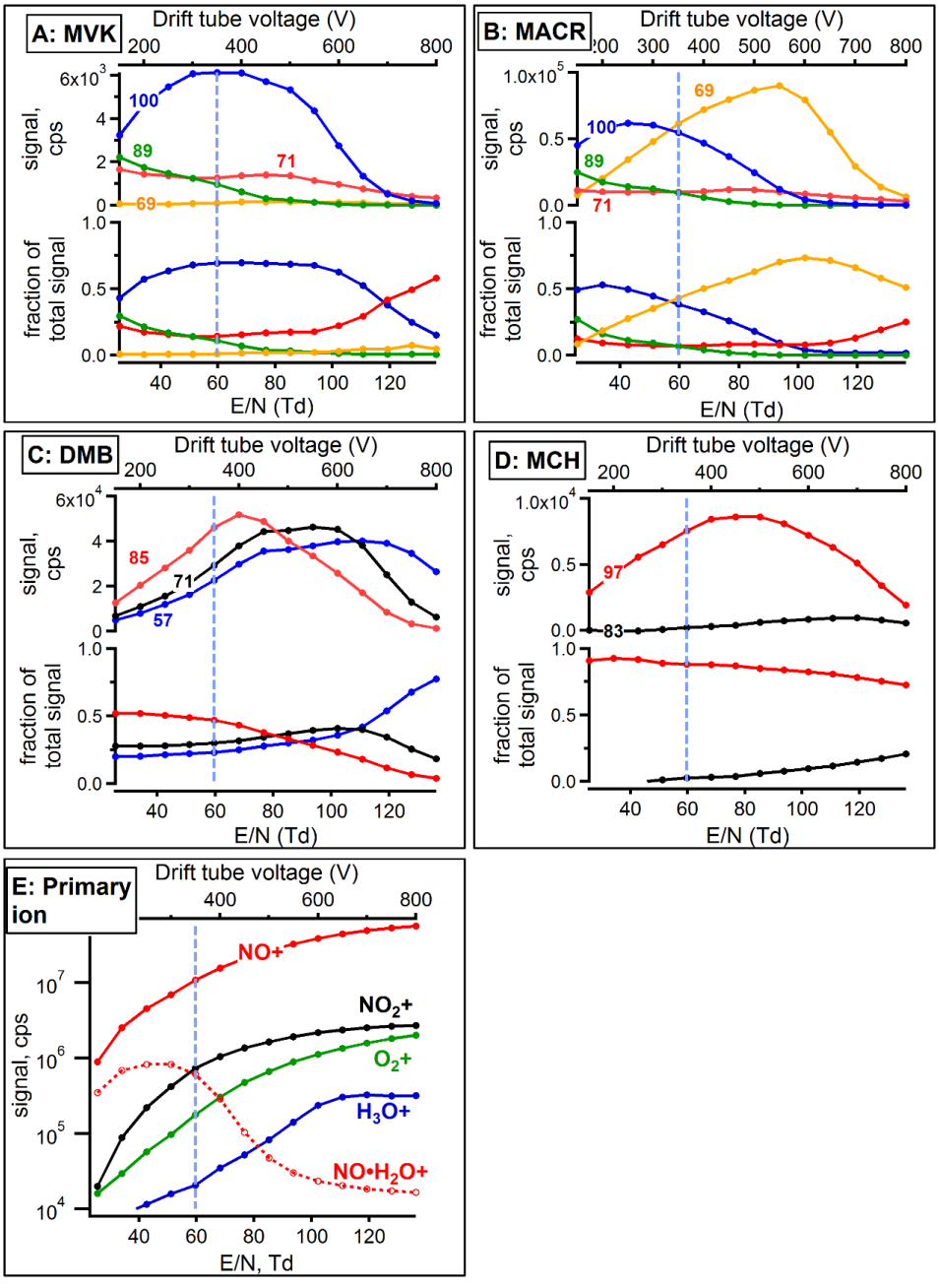

Figure 2. VOC and primary product ion dependence on drift tube voltage. Traces are labeled by the nominal product ion m/z in Th. (a) Methyl vinyl ketone. (b) Methacrolein. (c) 2,2-dimethylbutane. (d) Methylcyclohexane. (e) Primary ions and clusters. The dashed line indicates the selected operating voltage.

Atmos. Meas. Tech. Discuss., doi:10.5194/amt-2016-78, 2016
Manuscript under review for journal Atmos. Meas. Tech.
Published: 7 April 2016

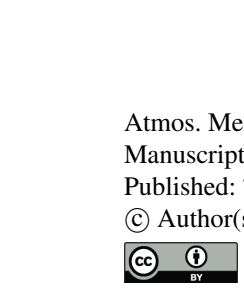

Atmospheric Measurement Techniques Discussions

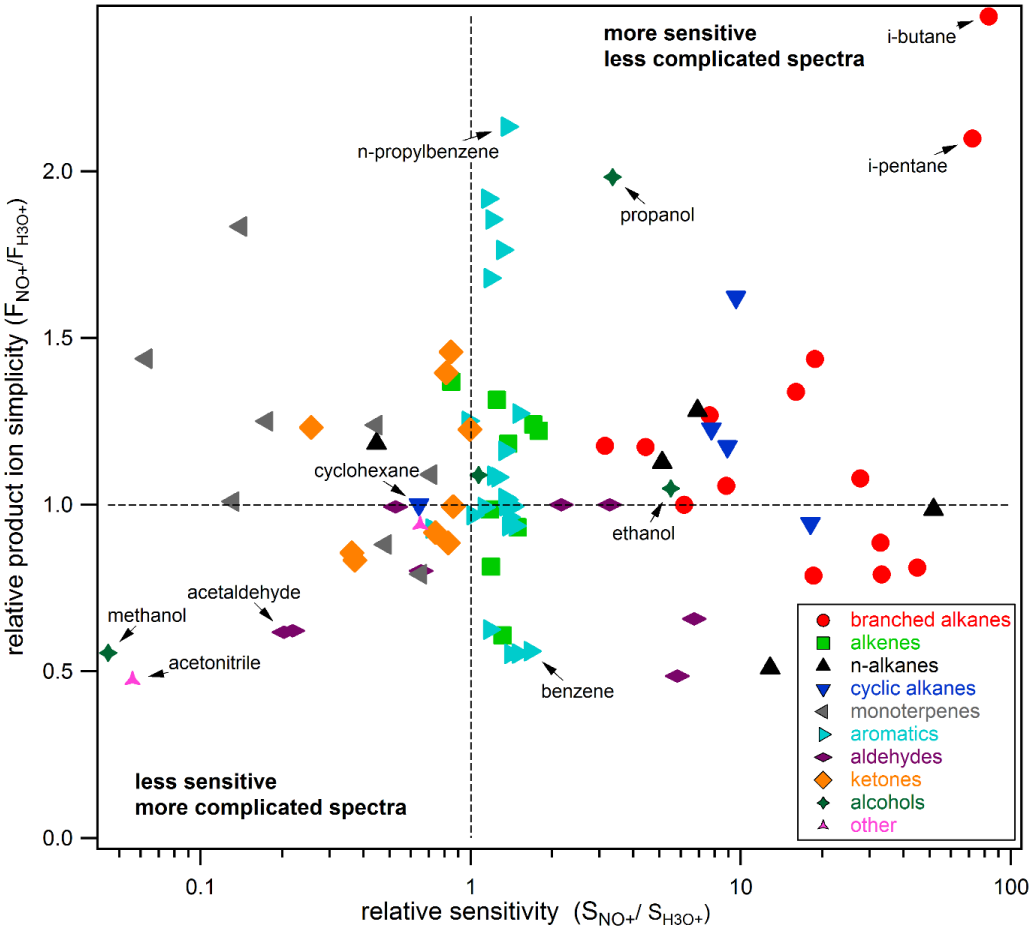

Figure 3. Comparison of production ion distribution and sensitivity of VOCs using NO^+ and H_3O^+ reagent ion chemistry.

Atmos. Meas. Tech. Discuss., doi:10.5194/amt-2016-78, 2016
Manuscript under review for journal Atmos. Meas. Tech.
Published: 7 April 2016

Atmospheric Measurement Techniques Discussions

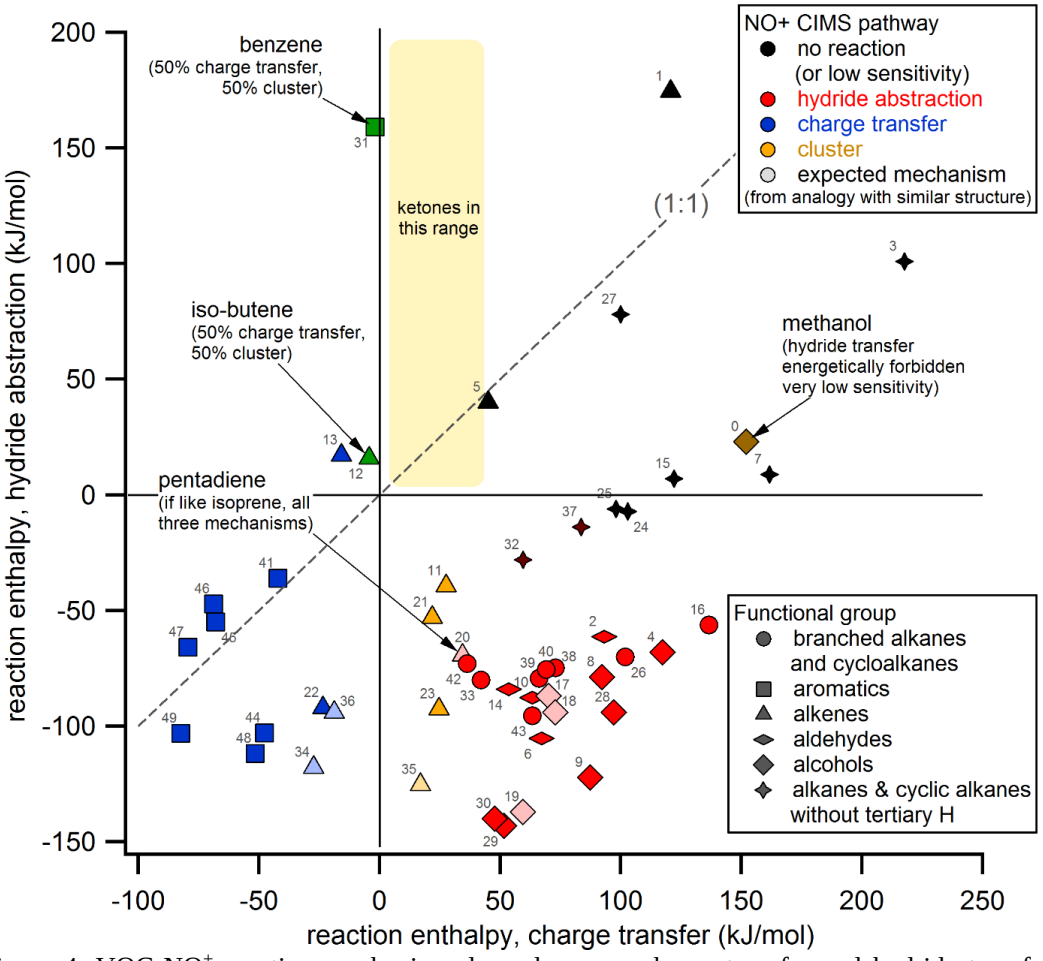

Figure 4. VOC-NO^+ reaction mechanism dependence on charge transfer and hydride transfer reaction enthalpy. VOC identification is indicated by the small numbers and is listed in Table 1. Hydride abstraction enthalpies for ketones are not known, but can be assumed to be positive based on structural considerations (lack of tertiary hydrogen). Ion thermodynamic information is available for several species whose reaction mechanism was not experimentally verified in this work; an expected mechanism was determined by analogy with a VOC of similar structure:
17 1-butanol; by analogy with 1-propanol.
18 2-methylpropanol; by analogy with 1-propanol.
19 2-butanol; by analogy with 2-propanol.
20 1,4-pentadiene; by analogy with isoprene.
34 4-methyl-2-pentene; by analogy with 2-pentene.
35 3-methyl-1-pentene; by analogy with 1-hexene.
36 2,3,-dimethyl-1-butene; by analogy with iso-butene.

Atmos. Meas. Tech. Discuss., doi:10.5194/amt-2016-78, 2016
Manuscript under review for journal Atmos. Meas. Tech.
Published: 7 April 2016

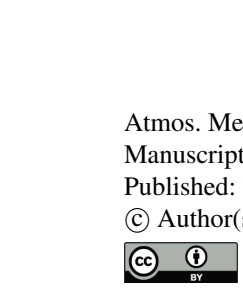

Atmospheric Measurement Techniques Discussions

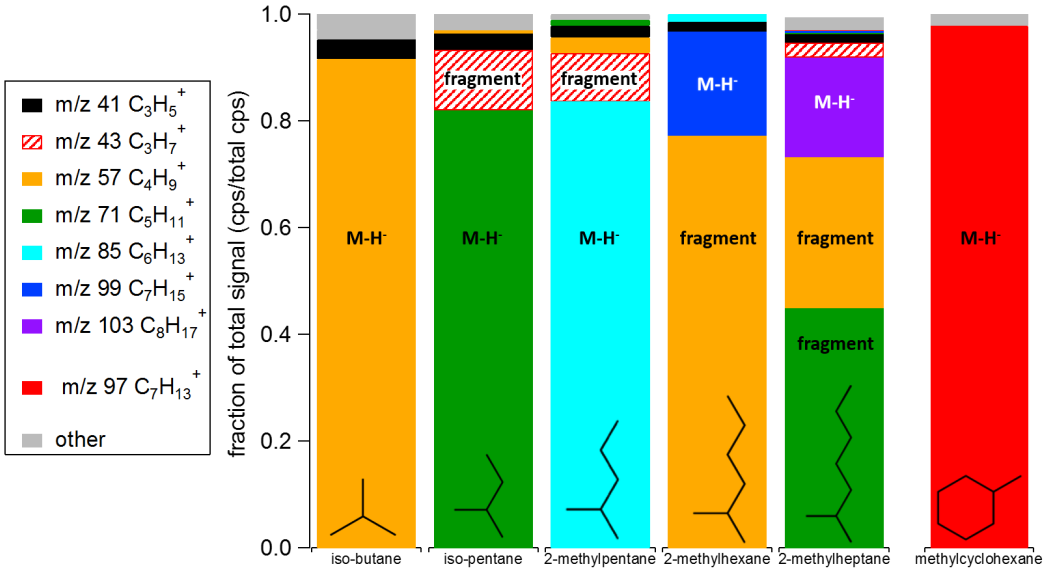

Figure 5. Product ion distributions of selected aliphatic hydrocarbons.

Atmos. Meas. Tech. Discuss., doi:10.5194/amt-2016-78, 2016
Manuscript under review for journal Atmos. Meas. Tech.
Published: 7 April 2016

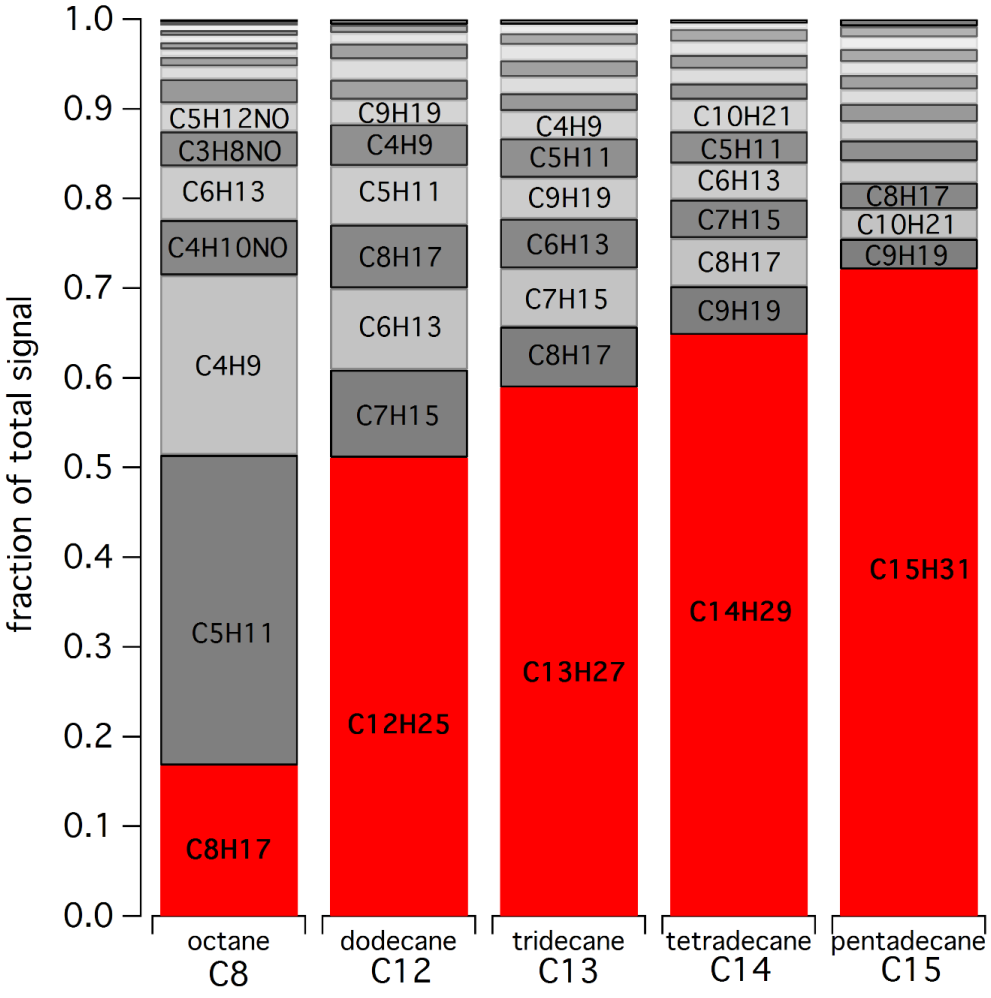

Figure 6. Large (C12-C15) n-alkane product ion distribution. The expected largest mass resulting from hydride abstraction (*m-1*) is highlighted in red. N-octane (C8) is shown for comparison.

Atmos. Meas. Tech. Discuss., doi:10.5194/amt-2016-78, 2016
Manuscript under review for journal Atmos. Meas. Tech.
Published: 7 April 2016

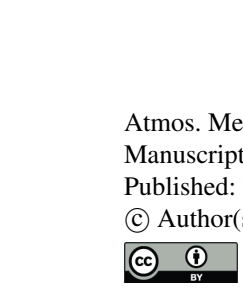

Atmospheric Measurement Techniques Discussions

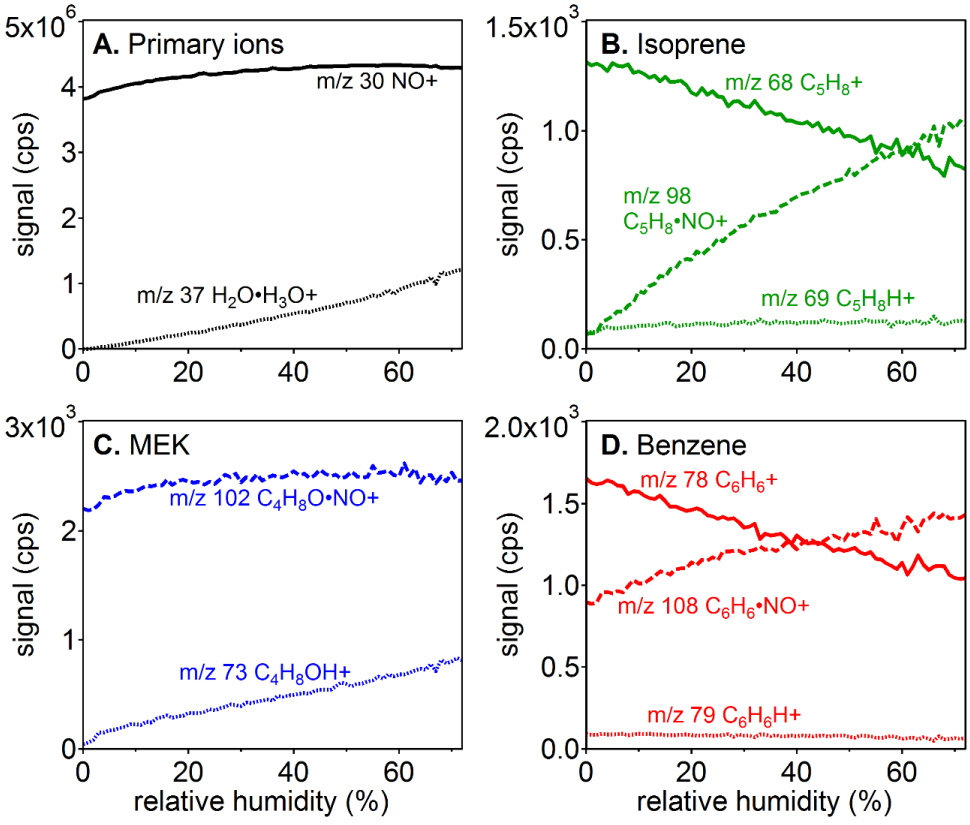

Figure 7. Humidity dependence of primary ions and selected VOCs. (a) NO^+ and water clusters. (b) isoprene. (c) methyl ethyl ketone (MEK). (d) benzene.

Atmos. Meas. Tech. Discuss., doi:10.5194/amt-2016-78, 2016
Manuscript under review for journal Atmos. Meas. Tech.
Published: 7 April 2016

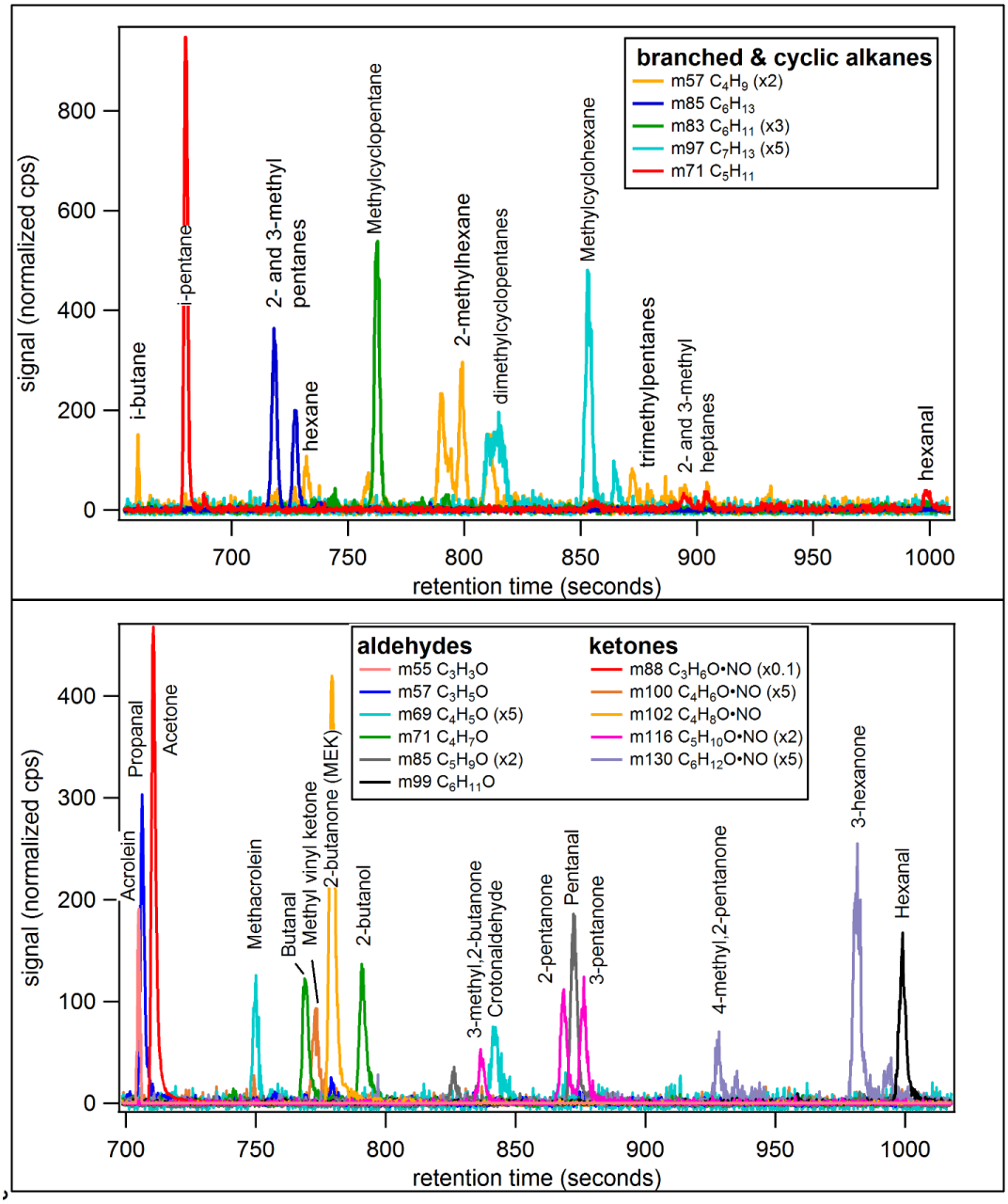

Figure 8. Example GC-CIMS chromatogram of ambient air sample. Masses have been split between two panels for clarity. Top: select masses corresponding to branched and cyclic alkanes. Bottom: select masses corresponding to aldehydes and ketones.

Atmos. Meas. Tech. Discuss., doi:10.5194/amt-2016-78, 2016
Manuscript under review for journal Atmos. Meas. Tech.
Published: 7 April 2016

Atmospheric Measurement Techniques Discussions

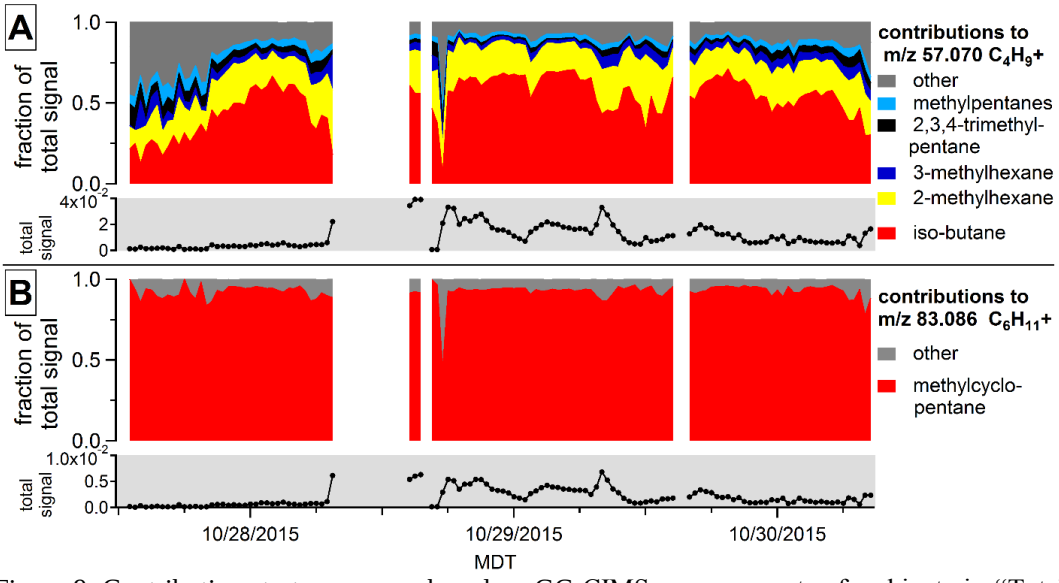

Figure 9. Contributions to two masses based on GC-CIMS measurements of ambient air. "Total signal" is normalized counts per chromatogram. (a) m/z 57 $C_4H_9^+$. (b) m/z 83 $C_6H_{11}^+$.

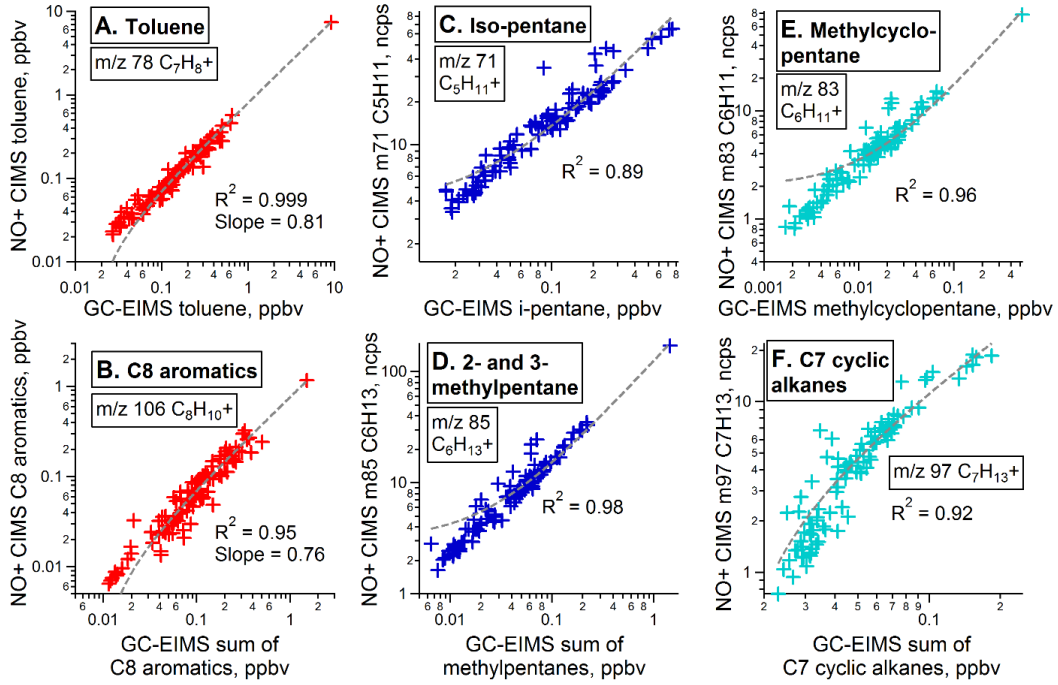

Figure 10. Correlations between VOCs measured with GC-EIMS and NO^+ ToF-CIMS. The 1Hz NO^+ ToF-CIMS measurement is averaged to the 5 minute GC collection period. Orthogonal least-squares linear best fits (ODR best fit) are shown with dashed lines. The lines appear curved due to log scale axes. For several compounds (e.g. methylcyclopentane, 2-and 3 methylpentanes), the

Atmos. Meas. Tech. Discuss., doi:10.5194/amt-2016-78, 2016
Manuscript under review for journal Atmos. Meas. Tech.
Published: 7 April 2016

Atmospheric Measurement Techniques Discussions

single high outlier pulls the best fit slightly away from the data points at low mixing ratios. (a) Toluene. (b) C8 aromatics: sum of ethylbenzene, o-xylene, m-xylene, and p-xylene. (c) Isopentane. (d) Sum of 2-methylpentane and 3-methylpentane. (e) Methylcyclopentane. (f) C7 cyclic alkanes: sum of methylcyclohexane, ethylcyclopentane, and dimethylcyclopentanes.

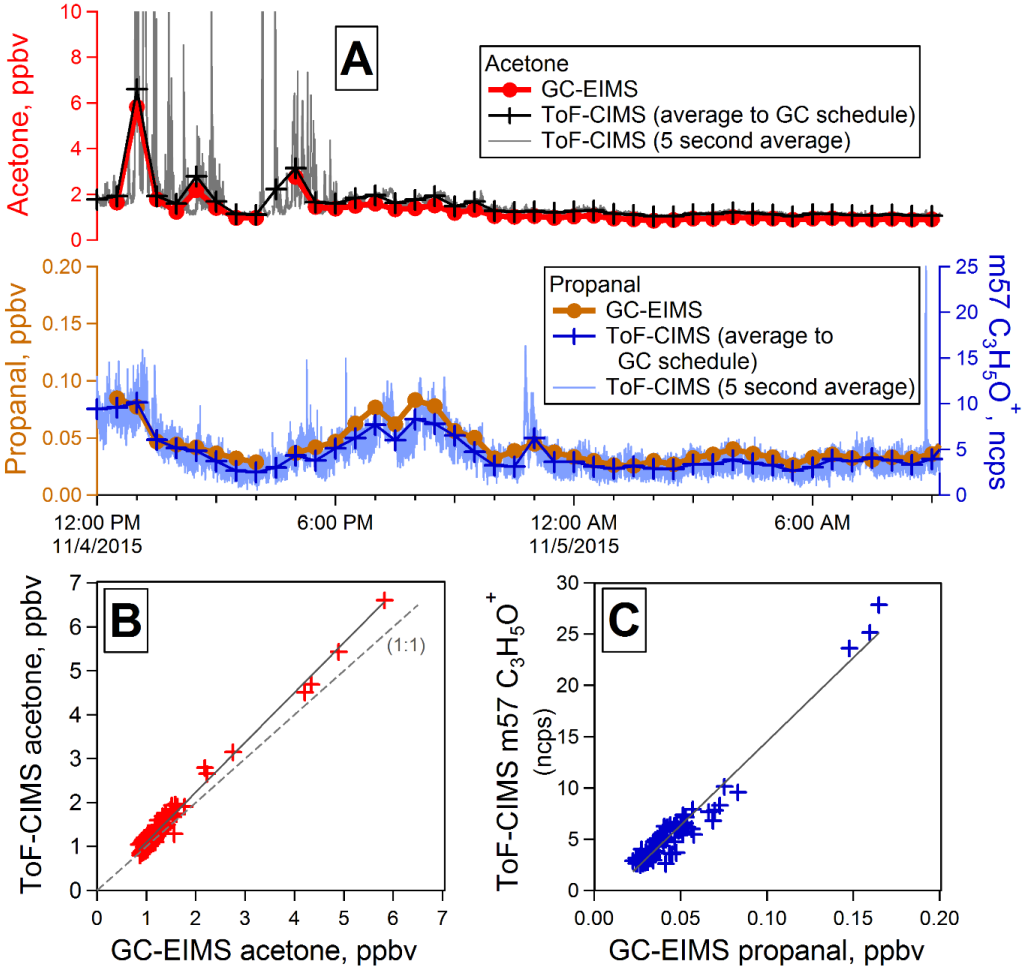

Figure 11. (a) Time series of acetone and propanal measurements from NO+ ToF-CIMS and GC-EIMS. Measurements shown include the GC-EIMS measurement (5 minute sample every 30 minutes, circle markers), the NO^+ ToF-CIMS measurement averaged over the five-minute GC sampling period (cross markers), and the NO+ ToF-CIMS measurement averaged to a 5 second running mean. (b) Correlation between NO^+ ToF-CIMS and GC-EIMS measurement of acetone. (c) Correlation between NO^+ ToF-CIMS and GC-EIMS measurement of propanal.

Atmos. Meas. Tech. Discuss., doi:10.5194/amt-2016-78, 2016
Manuscript under review for journal Atmos. Meas. Tech.
Published: 7 April 2016

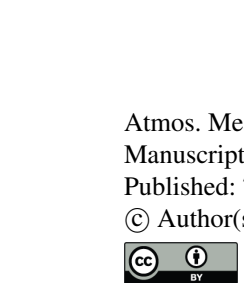

Atmospheric Measurement Techniques Discussions

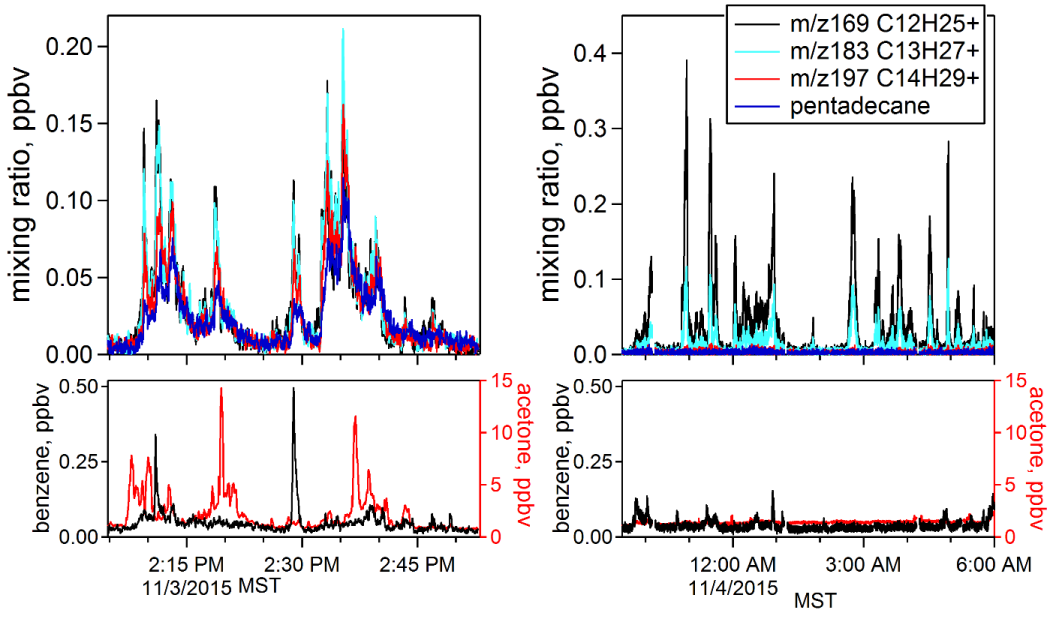

Figure 12. Episodes with elevated high-mass alkane masses. Mixing ratios for m/z 169 $C_{12}H_{25}^+$ (dodecane), m/z 183 $C_{13}H_{27}^+$ (tridecane), and m/z 197 $C_{14}H_{29}^+$ (tetradecane) are shown in approximate ppbv, assuming the same instrument calibration factor as pentadecane. Additional VOC species (benzene, acetone) are shown in the bottom panels for context.